JPL Blanket

jpl

CHANISM OF SUBCOOLED NUCLEATE

NAS 7-100

JET PROPULSION LABORATORY
CALIFORNIA INSTITUTE OF TECHNOLOGY
PASADENA, CALIFORNIA

MEMORANDUM NO. 30-8

ON THE MECHANISM OF SUBCOOLED NUCLEATE BOILING

S. G. BANKOFF

JET PROPULSION LABORATORY
CALIFORNIA INSTITUTE OF TECHNOLOGY
PASADENA, CALIFORNIA
FEBRUARY 5, 1959

National Aeronautics and Space Administration
Contract No. NASw-6

Memorandum No. 30-8

ON THE MECHANISM OF SUBCOOLED NUCLEATE BOILING

S. G. Bankoff

D. R. Bartz, *Chief*
Power Plant Research Section

Copy No. _____

JET PROPULSION LABORATORY
California Institute of Technology
Pasadena, California
February 5, 1959

CONTENTS

TABLES

FIGURES

PREFACE

Portions of the following report were originated under studies conducted for the Department of Army Ordnance Corps under Contract No. DA-04-495-Ord 18. Such studies are now conducted for the National Aeronautics and Space Administration under Contract No. NASw-6.

ABSTRACT

The mechanism of heat transfer in forced-convection subcooled nucleate boiling is considered. A three-step model is proposed. First, the heat flows from the wall into the adjacent liquid by two parallel paths: (a) the portion of the wall area which is periodically covered by bubbles is primarily cooled by quenching, due to colder liquid rushing in as the bubbles collapse; (b) over the remainder of the wall area, convective heat transfer is induced primarily by the stirring effect of the bubbles. Secondly, heat flows through the two-phase wall layer, partly by turbulent convection in the liquid between the bubbles, and partly by latent heat transport within the bubbles themselves. Finally, the heat flows by turbulent convection from the edge of the two-phase wall layer into the turbulent core. Simplified expressions are deduced for the first and third steps, which give reasonable agreement with Gunther's data. The relative importance of latent heat transport is as yet uncertain, but it is shown to be very likely significant in comparison with the heat flow through the liquid between the bubbles. Expressions are deduced for the quenching heat flux and and the mean velocity induced by the bubbles. The liquid temperature at the edge of the two-phase wall layer is computed for Gunther's data and is found to rise sharply towards the saturation temperature as burnout is approached. This signifies that the maximum heat flux coincides with the appearance of a fairly thick layer of warm water next to the wall, possibly due to the inability of the turbulent core liquid to remove the heat as fast as it is transmitted through the two-phase wall layer.

The heat flow expressions which have been derived are quite approximate; considerably more data on the local parameters in subcooled nucleate boiling are required before they can be put on a firm footing. On the other hand, the three-step model is not considered to be speculative; it is, in fact, a simple statement of the physical situation in highly subcooled nucleate boiling.

I. INTRODUCTION

It is the intent of this work to construct a potentially useful model for the heat flow in subcooled nucleate boiling. The model is limited to subcooled boiling, for the simple reason that the only reasonably complete data on bubble parameters are from Gunther's work on forced-convection subcooled boiling of water at essentially atmospheric pressure (see Ref. 1). Crude as this model necessarily is, in view of the severely limited quantity of experimental information, a number of interesting aspects are developed in its formulation; and it is hoped that its presentation will stimulate further quantitative measurements of the local parameters in boiling which are so sorely needed for a fuller understanding of this complex phenomenon.

II. PRELIMINARY CONSIDERATIONS

Nucleate boiling is characterized by the presence of favored locations for bubble formation, or nuclei, on the heating surface. Portions of the ebullition surface which are in the immediate neighborhood of a nucleus are periodically covered by bubbles, so that they are alternately in contact with vapor and then with liquid. On the other hand, portions of the ebullition surface which are at some distance from any nucleus will always be in contact with liquid. It is evident that the heat transfer from these two portions of the surface proceeds by different mechanisms, so that one may write:

$$q_t = q_u^* f + q_w^* (1 - f) = q_u + q_w \tag{1}$$

where q_t is the total heat flux, f is the fraction of the surface which is periodically in contact with bubbles, q_u is the heat flux from this portion of the surface, and q_w is the heat flux from the remainder of the surface. The star symbol denotes that the heat flux is calculated on the basis

of the actual heat-transfer surface, whereas the absence of a star denotes that it is calculated on the basis of the total wall area.

Alternatively, one may write, at any instant:

$$q_t = q_b^* F + q_c^*(1 - F) = q_b + q_c \tag{2}$$

where q_b is the heat flux from the surface beneath the bubbles, q_c is the convective heat flux from the surface between the bubbles at any instant, and F is the instantaneous fraction of the surface covered with bubbles. Here F is a stochastic variable; but, if a large enough heating surface is employed, the space-mean fraction of the surface covered may be equated to the time-mean fraction of the surface covered, in accordance with the ergodic hypothesis (see Refs. 2 and 3). It should be carefully noted that these equations apply to the heat transfer from the wall to the inner portion of the two-phase wall layer, which is here arbitrarily defined to be the layer next to the wall of thickness equal to R_m, the mean maximum bubble radius. (See Fig. 1.) The flow from the inner to the outer portion of the layer is quite distinct from that of the outer portion of this layer to the turbulent core liquid.

It is usually considered that

$$q_b << q_c \tag{3}$$

since heat-transfer coefficients from solids to gases are very much less than those from solids to liquids. In this sense each bubble is considered to be an insulating spot on the wall surface.

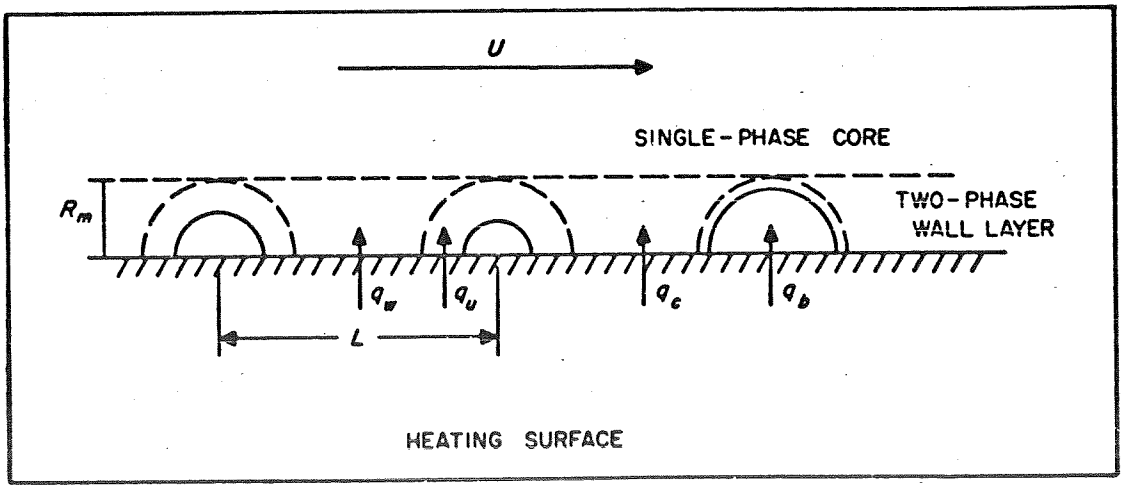

Fig. 1. Diagrammatic Sketch of Heat Flow from Wall into Two-Phase Layer

This may not be strictly true if there is an appreciable liquid film at the base of each bubble. (See Ref. 4.)

Rannie is said (Ref. 5) to have called attention to the fact that a principal mode of heat transfer may result from the periodic contact of relatively cold liquid with dry spots which were formerly covered by bubbles. To express this quantitatively, it may be noted that at any instant the fraction of the surface which was formerly dry, and is now in contact with quenching liquid, is $(f - F)$. From the portion of the surface which is never covered by bubbles, convective heat flow dominates. Hence, considering Eqs. (2) and (3),

$$q_t \sim q_c^*(1 - F) = q_q^*(f - F) + q_w^*(1 - f) = q_q + q_w \tag{4}$$

can be obtained.

Heat flows from the inner to the outer portion of the two-phase wall layer will be denoted by the superscript 1 and thence to the turbulent single-phase core liquid by the superscript 2.

Then, the heat flow through the two-phase wall layer may be written

$$q_t = q_t^{(1)} = q_b^{(1)} + q_c^{(1)} \tag{5}$$

where $q_b^{(1)}$ is the heat flux due to vaporization of liquid at the inner portion of the wall layer and condensation at the outer portion; and $q_c^{(1)}$ is the convective heat transport through the liquid between the bubbles. It has been frequently stated that

$$q_c^{(1)} >> q_b^{(1)} \tag{6}$$

but, as will be shown, the evidence for this hypothesis is not conclusive. Actually, probably neither of these heat fluxes is negligible.

Finally, the convective heat flux from the outer portion of the two-phase wall layer to the turbulent single-phase core may be written

$$q_t = q_t^{(2)} = q_c^{(2)} \tag{7}$$

Tsien is said (Ref. 6) to have pointed out that the bubbles act as roughness elements in increasing both fluid friction and heat transfer. The interaction of the bubbles and the flowing stream determines $q_c^{(2)}$ in Eq. (7).

An attempt will be made to formulate expressions for these heat fluxes. Before entering upon this task, however, it is advisable to review the question of the relative magnitudes of the latent heat transport and the convective heat flux between the bubbles (Eq. 6).

III. LATENT HEAT TRANSPORT VS STIRRING

Several investigators (Refs. 7 and 8) have observed that the rate of visible vapor evolution in subcooled nucleate boiling can account for only a small fraction (1 to 2%) of the total heat flux. If it is assumed that the bubbles are surrounded by a stagnant laminar film as they grow and collapse, it can also be shown that mass flow within the bubbles, due to simultaneous vaporization at the equator and condensation at the pole, is also a second-order effect. It is not true, however, that the heat flow from the bubble condensing surfaces is dominated by laminar conduction through a stagnant film. Bankoff and Mikesell (Refs. 9 and 10) have extended the laminar Plesset-Zwick bubble growth solution (Ref. 11) to include an initially nonuniform temperature distribution around the bubble; the resulting solution can be fitted closely to saturated surface boiling data, but not to subcooled boiling. It is further pointed out that the time-irreversibility inherent in the laminar-heat-conduction equation is inconsistent with the symmetrical growth and collapse periods observed in highly subcooled nucleate boiling. If it is assumed, however, that turbulent and convective heat transfer dominates in removing heat from the condensing bubble surfaces, predictions can be made which are in good agreement with the trends exhibited by Gunther's and Ellion's data (Refs. 1 and 12). From well-known empirical equations for the heat-transfer coefficient of a single sphere suspended in a turbulent stream (Ref. 13) it is estimated that the latent heat transport represents at least 10% of the total heat flux. Measurements of turbulent-heat-transfer coefficients from single and multiple bubbles are needed to resolve tl uncertainty.

Another simple argument can be adduced to show that the stirring effect of the bubbles does not account for all of the heat flux. As more surface nuclei become active, upon increasing the surface temperature, the bubble population and the stirring effect of the bubbles increase. Hence, the total heat flux increases, even though more of the surface is covered at any time by bubbles, which act essentially as insulating spots. As the bubble population continues to increase, a point is reached where the increased heat flux due to stirring is just offset by the decrease in the instantaneous wetted area of the surface. This represents the maximum nucleate boiling heat flux, popularly called "burnout." The more rapidly the bubbles grow, the more vigorous will be the stirring, and the greater will be the maximum flux. However, the maximum flux in saturated pool boiling increases with pressure up to a reduced pressure of about 0.35 (Ref. 14), even though the mean bubble wall velocity decreases continuously with increased pressure. This means that the stirring effect of the bubbles is not the sole controlling factor. Significantly, we may note that the volumetric latent heat content of the vapor ($\lambda \rho_v$, where λ is the latent heat and ρ_v is the density of the vapor) has a maximum in the range of reduced pressures of 0.3 to 0.7.

This latter observation can be expanded by a simple calculation. It is instructive to estimate the vapor flow which would result if the equatorial and polar regions of the bubbles

could be maintained at different wall temperatures, by whatever mechanism. Plesset's solution (Ref. 15) of the problem of the steady-state one-dimensional flow of vapor between two liquid surfaces held at different temperatures is employed. The heat flux due to flow of vapor between a warm liquid surface at temperature T_0, and a colder surface at temperature, T_2, is given by:

$$q_v^* = \frac{q_v}{F} = \epsilon \lambda \rho_{0v} \left(\frac{R_G T_0}{2\pi M}\right)^{1/2} \left[1 - \left(\frac{\rho_{2v}}{\rho_{0v}}\right)\left(\frac{T_2}{T_0}\right)\right]\left[1 + \left(\frac{T_2}{T_0}\right)^{1/2}\right]^{-1} \tag{8}$$

where ϵ is the accommodation coefficient, λ is the latent heat, M is the molecular weight of the vapor, and ρ_{0v} and ρ_{2v} are the equilibrium or saturation vapor densities at the liquid surface temperatures, T_0 and T_2, respectively. For this rough calculation, it is assumed that the vapor transport can be satisfactorily approximated by a one-dimensional calculation and that the evaporative zone, near and at the base of the bubble, is about equal in area to the condensing zone near the polar cap. Temperature T_0 may be greater than T_2 for several reasons: (1) a thin liquid film may separate the spreading bubble from the wall (Ref. 4), (2) the expanding bubble receives a continuous new supply of superheated liquid near its base, and (3) the polar cap is cooled by turbulent convection. For this illustration, assume T_0 to be equal to the wall temperature, T_w, and T_2 to be equal to the saturation temperature T_{sat}. Cichelli and Bonilla (Ref. 14) have measured the wall superheat and heat flux at maximum pool nucleate boiling rates for five organic liquids. Their data for the wall superheat are closely approximated by an expression of the form

$$\Delta T_w = -45 \log_{10} p_r \tag{9}$$

where p_r is the reduced pressure of the system. Equations (8) and (9) were used to calculate q_v for pentane, assuming $\epsilon = 1$ and $F = 0.005$ (the latter choice is quite arbitrary, and is intended to fit the data. Its smallness, however, is significant, since at maximum flux at least one-third of the surface is covered with bubbles). The results are shown in Fig. 2. It is seen that Eq. (8) exhibits the same characteristic maximum burnout flux as the data and can be made to fit these data quite closely. Calculations for other organic liquids give similar behavior. This crude calculation is not intended to suggest that all the heat at maximum heat flux conditions is transported as latent heat; but it does strongly suggest that this mode of heat transport is not insignificant.

Finally, some interesting analogies to nucleate boiling may be examined which may shed some light on this subject. A parallelism between nucleate boiling and a diffusion-controlled

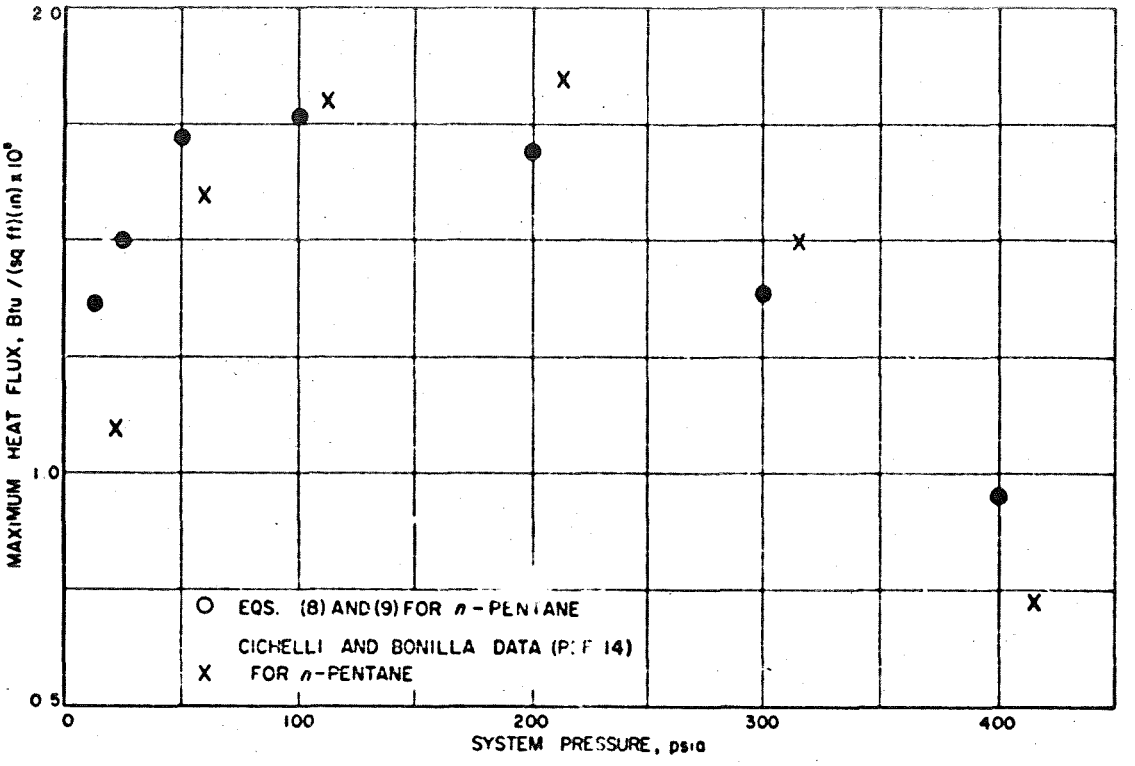

Fig. 2. Maximum Heat Flux in the Pool Boiling of *n*-Pentane: Data of Cichélli and Bonilla (Ref. 14) Compared with Eq. (8)

mass-transport phenomenon was found by Roald and Beck (Ref. 16). They rotated a cylindrical magnesium specimen in hydrochloric acid of various concentrations and measured the dissolution rate as a function of angular velocity. Beyond a certain acid concentration, hydrogen-bubble evolution on the surface became vigorous and resulted in sharply increased mass transfer rates. The authors attributed the increased rate to the stirring action of the hydrogen bubbles. The analogy to nucleate boiling appears to be excellent. In fact, one can imagine liquid which is not supersaturated with hydrogen gas being brought discontinuously in contact with the surface (quenching) by removal of bubbles from the surface; or that the bubbles act as roughnesses in increasing both frictional drag and mass transfer; or that the formation of hydrogen bubbles, through mass transport of vapor, provides an efficient means of reducing the degree of supersaturation of hydrogen gas in the liquid at the solid surface. In this connection, it should be noted that the analogy here is to saturated boiling, since the hydrogen bubbles (presumably) did not collapse on the surface. In steady-state saturated boiling all of the heat leaves the system as latent heat. Similarly, most of the hydrogen transport from the surface may well have been accounted for as hydrogen bubbles.

A more instructive analogy, which appears to have been overlooked, is dropwise condensation of vapors vs heat transfer from noncondensable gases. The heat-transfer coefficients in the

former case are of the order of hundreds of times greater than in the latter case (Ref. 17); but in this case the liquid droplets grow slowly, so that they cannot be considered to agitate the vapor near the wall very much (at least in comparison with the agitation required to obtain equal heat transfer in a noncondensing gas-solid system). Eucken (Ref. 18) attributes the increased heat-transfer rate to the reduction of the thickness of the layer of supercooled vapor near the surface by diffusion into the droplets.

One cannot attribute the increased heat-transfer coefficients once condensation begins, solely, or even primarily, to the stirring effect of the droplets; in fact, a small amount of non-condensable gas in the vapor reduces the heat transfer enormously, as is well-known. Eucken's explanation appears to be a reasonable one. In the same way that the droplet surfaces act as concentration sinks for diffusion of supercooled vapor, one may expect that the nucleate boiling bubbles act as distributed temperature sinks for the diffusion of heat from the superheated liquid layer adjacent to the wall.

From the preceding discussion, despite the widely-held concepts of the bubbles acting principally as turbulence promoters, one is forced to conclude that the direction of the inequality (Eq. 6) is uncertain. Probably both latent heat transport within the bubbles and convective transport between the bubbles are important.

IV. CHARACTERISTIC BUBBLE QUANTITIES

A. Quenching Heat Flux

Before preceding with the task of formulating expressions for the heat flow, it will be convenient to derive several characteristic bubble quantities which will be needed later. One of these is the heat flux, q_q, due to the quenching of dry spots on the wall.

When a bubble collapses in subcooled boiling, or when it leaves the surface in saturated boiling, relatively cold liquid comes into contact with what was formerly an essentially dry spot on the wall. The following assumptions are made:

1. The flow of heat from the wall into the liquid is perpendicular to the wall.
2. The liquid which comes into contact with the wall is at a uniform temperature.

These assumptions are equivalent to replacing, for the short time periods involved, the incoming liquid by a sequence of thin annular lamina, of radius $R = R(t)$ and thickness dR, at a time t after the bubble begins to grow (Fig. 3). These lamina are initially at a uniform temperature, say $T_1 \leq T_{sat}$, characteristic of the liquid immediately above the bubbles. The wall is initially at the mean wall superheat temperature T_w, variations in the wall temperature being ignored in this approximation. For subcooled boiling, the problem can be formulated in terms of the average bubble lifetime, θ, and period, θ', as follows: Let

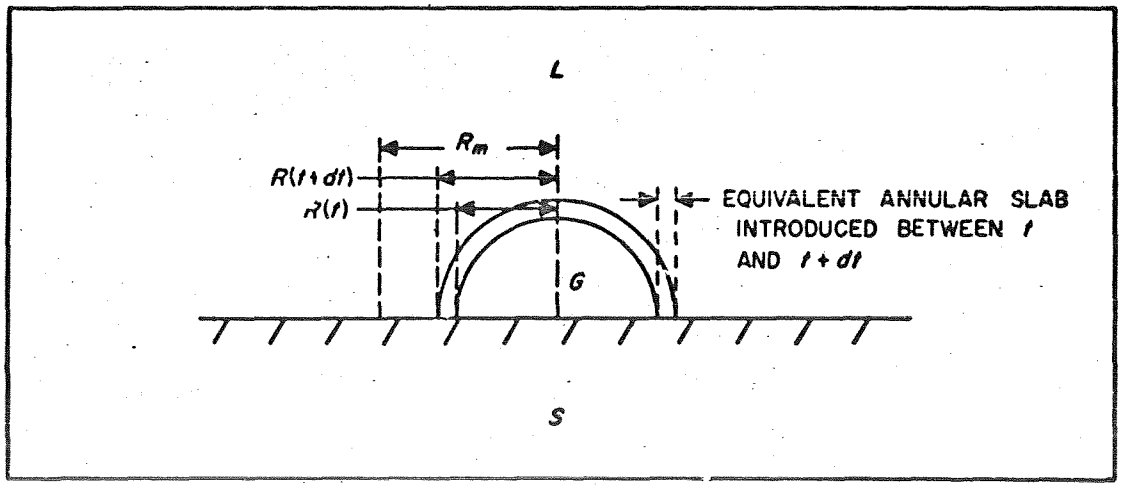

Fig. 3. Model for Calculation of Quenching Heat Flux upon Collapse of a Single Bubble

$$R(0) = 0, \quad R\left(\frac{\theta}{2}\right) = R_m, \quad R(t) = 0, \quad \theta \leq t \leq \theta' \tag{10}$$

since no bubble is present at times between θ and θ'. At time t, a new segment of area $2\pi R(t)\,dR$, is placed in contact with the hot surface, where $\theta/2 < t < \theta$. The temperature in this slab at time θ' is

$$T - T_w = (T_1 - T_w)\,\mathrm{erf}\left(\frac{y}{2\sqrt{\alpha(\theta' - t)}}\right) \tag{11}$$

where T is the temperature at a distance y from the wall, and α is the thermal diffusivity of the liquid. This is the well-known solution for the temperature of a uniform, semi-infinite slab subjected to a step change in temperature on its surface.

The heat content of the slab is

$$dH = 2\pi\rho_L C_L R(t) \mid dR \mid (T_w - T_1) \int_0^\infty \mathrm{erfc}\left(\frac{y}{2\sqrt{\alpha(\theta' - t)}}\right) dy \tag{12}$$

$$= 4\rho_L C_L R(t) \mid dR \mid (T_w - T_1)\sqrt{\pi\alpha(\theta' - t)}$$

The total heat content of the liquid due to heat conduction upon collapse of one bubble is

$$H = \int_0^H dH = -4\rho_L C_L \sqrt{\pi\alpha}\,(T_w - T_1) \int_{\theta/2}^{\theta} R(t)\,\dot{R}(t)\sqrt{\theta' - t}\,dt \tag{13}$$

where the dot denotes differentiation with respect to time. Then, the total heat flux due to this quenching mechanism is given by

$$q_q = NH \tag{14}$$

where N is the number of bubbles forming on the surface per unit area per unit time.

It remains, therefore, to find a suitable expression for $R = R(t)$. Gunther, in calculating F, the time-average fraction of the surface covered by bubbles, was able to approximate the integral

$$\int_0^\theta R^2 dt \simeq 0.57\, R_m^2 \theta \tag{15}$$

within the accuracy of the data, or about ±5%. Noting the near symmetry of the growth and collapse regions in subcooled boiling, a parabolic approximation is tried, satisfying the boundary conditions (Eq. 10)

$$\left.\begin{aligned} 1 - s &= (\zeta - 1)^2 \qquad 1 \le \zeta \le 2 \\ s &= 0 \qquad\qquad\quad 2 \le \zeta \le 2K \end{aligned}\right\} \tag{16}$$

where

$$s = \frac{R}{R_m}, \quad \zeta = \frac{2t}{\theta}, \quad \text{and} \quad K = \frac{\theta'}{\theta} \tag{17}$$

The integral (Eq. 15) then becomes

$$\int_0^\theta R^2 dt = \frac{R_m^2 \theta}{2} \int_0^2 s^2 d\zeta = 0.533\, R_m^2 \theta \tag{18}$$

within 6.5% of the approximation (Eq. 15). This is considered to be satisfactory for the present purpose. It may be noted that a sine approximation,

$$s = \sin \frac{\pi \zeta}{2}$$

is not as satisfactory, giving a value for the integral (Eq. 15) of $0.5\, R_m^2 \theta$.

Substituting Eq. (16) in Eq. (13)

$$H = -B \int_1^2 s(\zeta)\, \dot{s}(\zeta)\, \sqrt{2K - \zeta}\, d\zeta \tag{19}$$

$$= 2B \int_0^1 (1 - \xi^2)\, \xi \sqrt{b - \xi}\, d\xi \tag{20}$$

$$= B\, \psi(K) \tag{21}$$

where

$$\psi(K) = \frac{8}{315} \left[(8b^4 + 4b^3 - 18b^2 - 8b + 14)\sqrt{b - 1} - (8b^4 - 21b^2)\sqrt{b} \right] \tag{22}$$

and

$$B = \sqrt{8\pi\alpha\theta}\, \rho_L C_L (T_w - T_1)\, R_m^2; \quad \xi = \zeta - 1; \text{ and } b = 2K - 1 \tag{23}$$

A plot of $\psi(K)$ is given in Fig. 4. Substituting Eqs. (21) and (23) in Eq. (14),

$$q_q = 5.01\, N (T_w - T_1)\, R_m^2 \sqrt{\rho_L C_L k_L \theta}\, \psi(K) \tag{24}$$

Actually, the bubble slides along the wall as it grows and collapses. Hence, the area swept out by the bubble base, instead of being a circle, of radius R_m, is roughly an ellipse, the minor semi-axis of which is R_m. If the bubble axis is assumed to travel downstream at 0.8 the free-stream velocity (Ref. 1), the major semiaxis is approximately $R_m + 0.4\, V\theta$. Using the ratio

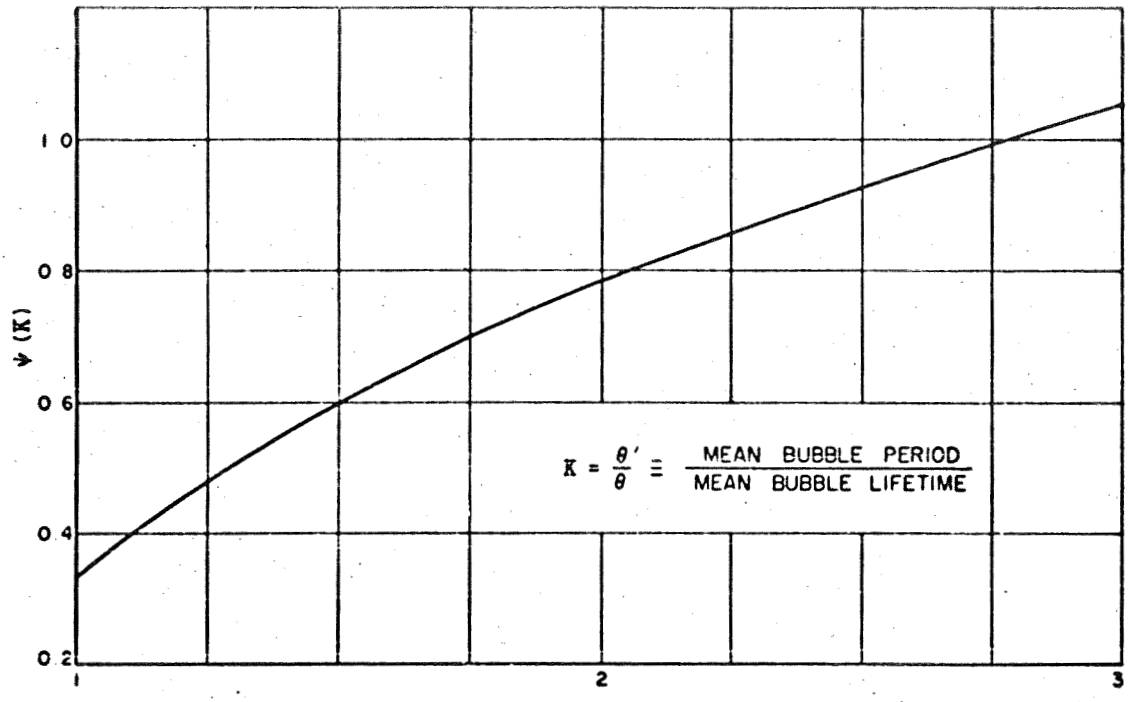

Fig. 4. Plot of ψ (K), Eq. (22), vs K

of the areas as a correction factor, Eq. (24) gives

$$q_q = 5.01\, N(T_w - T_l)\, R_m^2 \sqrt{\rho_L C_L k_L \theta}\, \psi(K) \left[1 + \frac{0.4V\theta}{R_m}\right] \tag{25}$$

B. Root-Mean-Square Velocity Between Bubbles

The time-average fraction of the surface covered by bubbles is assumed to be constant (steady-state boiling). If the liquid is sufficiently subcooled, the bubble radius-time curve is symmetrical, corresponding to growth and collapse curves which are mirror images of each other (Ref. 1). In this event the number of bubbles collapsing at any instant will equal the number growing; and it is possible to assign each growing bubble, which acts as a velocity source, to a neighboring collapsing bubble, or velocity sink. If viscous effects are neglected, the system at any instant can be considered to be a coplanar assembly of sources of velocity potential, each of

which has associated with it an equal sink. Two cases may be considered: (1) the distance between centers L is large compared to the average radius of the bubbles R_a, in which case the bubbles may be considered to be point sources or sinks; and (2) L is of the same order of magnitude as R_a.

In the former case, the velocity potential at any point P is given by summing the contributions from each of the sources and sinks:

$$\phi_P = \sum_i \phi_i = \sum_i \frac{m_i}{r_i} \tag{26}$$

where m_i, the strength of the ith source, is equal to $(R^2\dot{R})_i$ and r_i is the magnitude of the radius vector r_i from the ith source to P (Fig. 5). If, in addition, a uniform stream velocity V in the negative x direction is superimposed, Eq. (26) becomes

$$\phi_P = \sum_i \frac{(R_2\dot{R})_i}{r_i} + Vx \tag{27}$$

The velocity at P is

$$\vec{u}_P = -\nabla\phi_P = -\sum_i \frac{(R^2\dot{R})_i \vec{r}_i}{r_i^3} - V\vec{i} \tag{28}$$

where $\vec{i}$ is the unit vector in the x direction. The corresponding two-dimensional problem can be solved exactly (see Appendix); but for our present purposes, some simple qualitative considerations are sufficient. Suppose the sources and sinks to be moved closer together, while keeping their strengths and relative positions the same. If the external velocity V is small compared to the velocity due to the bubbles, the velocity at P will vary as the inverse square of the distance between centers. The dependence becomes less strong as V becomes relatively larger, until when V is very large compared with the velocity induced by the bubbles, the distance between centers has no effect.

It is rarely if ever true, however, that the radius of the bubbles is negligible compared with the distance between centers. Assume now that the bubbles form a square net, that K = 1,

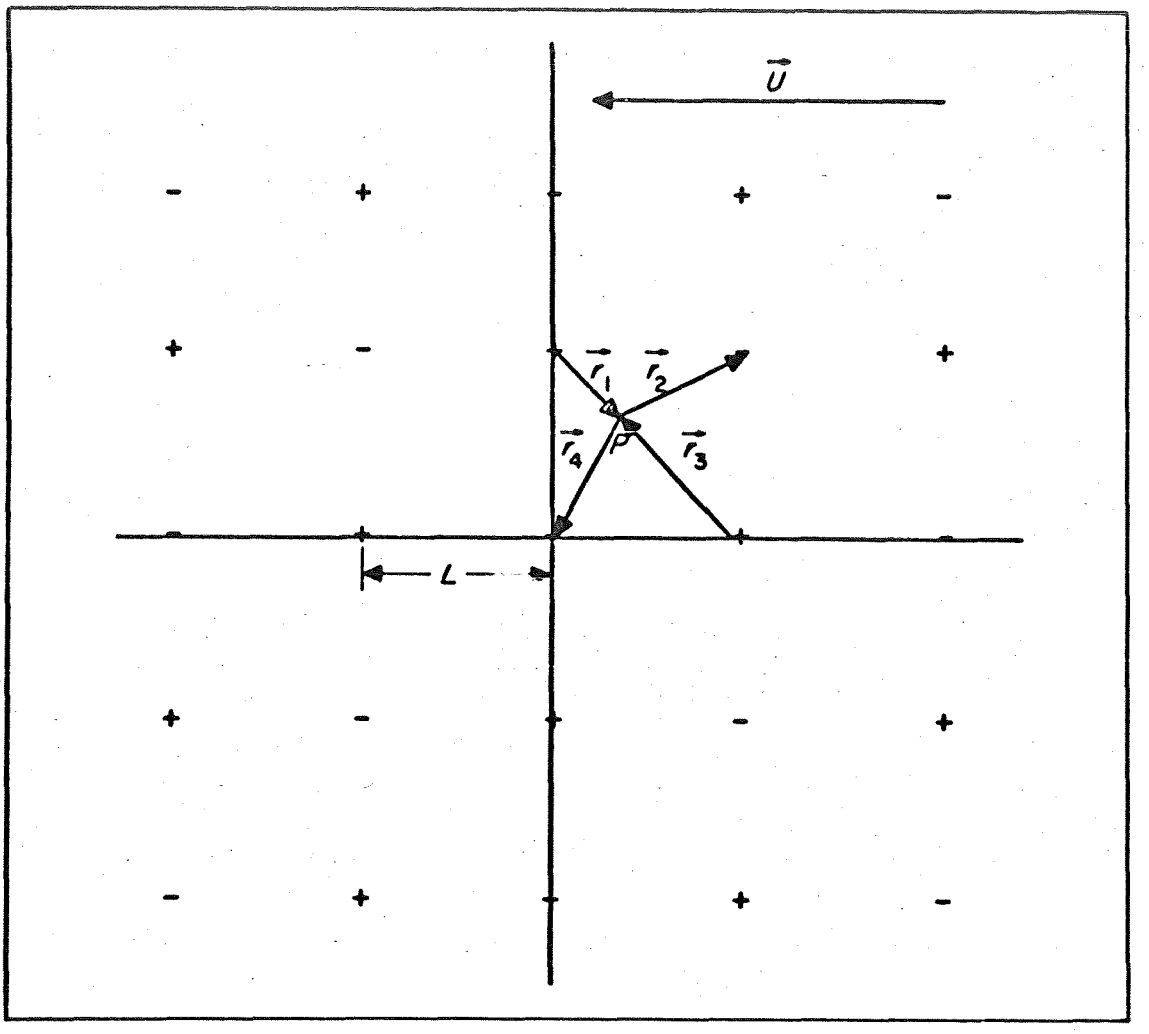

Fig. 5. Model of Assembly of Bubbles Growing and Collapsing on a Surface. Distance Between Centers L Large Compared with Mean Bubble Radius R_a. Square, In-Line Net

and since the growth and collapse curves are symmetrical, that the radius of every bubble, $R_a = \frac{1}{2} R_m$. Hence, the growth rate is either $\pm \dot{R}_a$. Confining attention to a unit cell of this net, given by the perimeter *ABCDEFGH* (Fig. 6), consider a thin lamina of liquid in contact with the heating surface, area of which is defined by the above perimeter. Since all velocities normal to the solid surface are very small in this lamina, it may be assumed that all flow across the boundaries occurs at the perimeter. The kinetic energy of the liquid within the lamina (Ref. 19) is

$$\frac{1}{2} \rho_L \int u^2 d\eta = - \frac{1}{2} \rho_L \int \phi \frac{\partial \phi}{\partial n} dS \qquad (29)$$

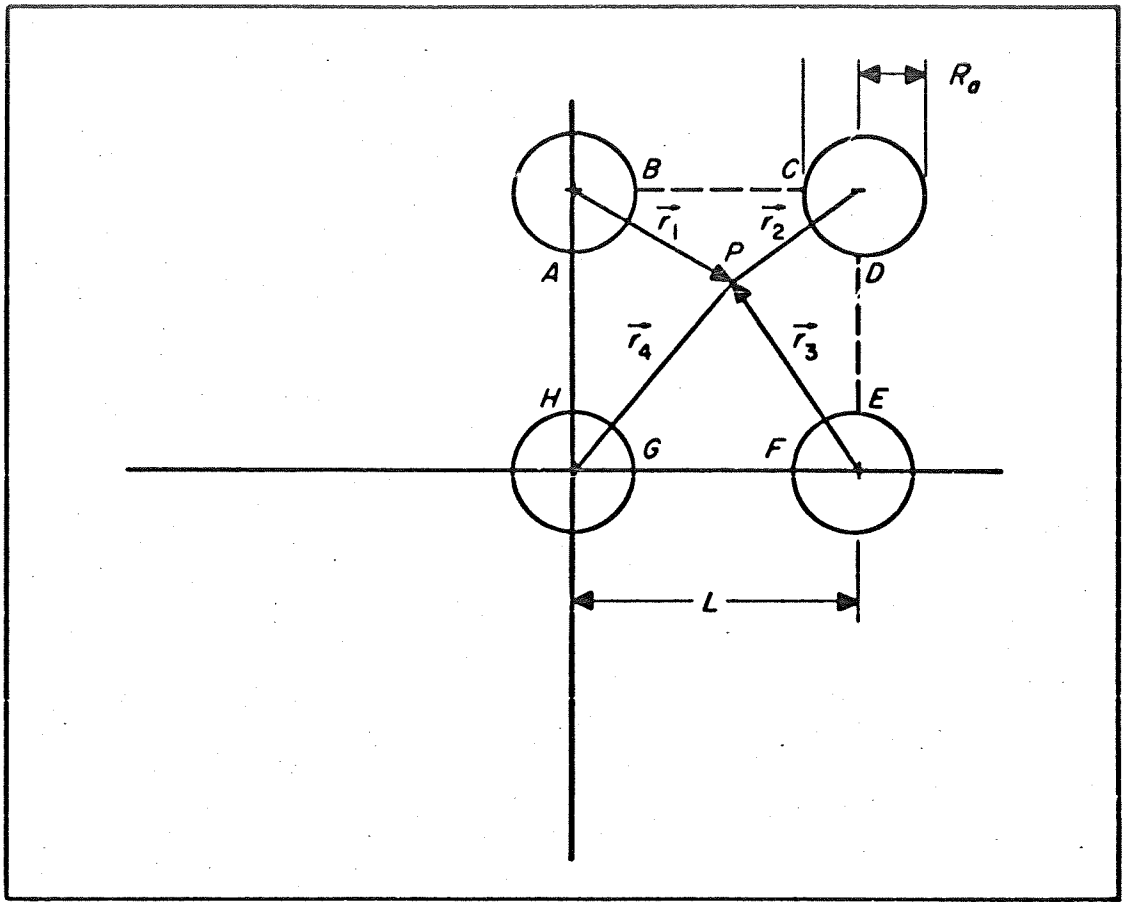

Fig. 6. Model of Assembly of Bubbles Growing and Collapsing on a Surface. Distance Between Centers L Compared with Mean Bubble Radius R_a. Square, In-Line Net

where ρ_L and u are density and velocity, respectively, and $d\eta$ and dS are volume and surface elements. The normal velocity across the boundary, $-\partial\phi/\partial n$, vanishes by symmetry over the perimeter elements BC, DE, FG, and HA. Over the remaining portions of the boundary it is essentially $\pm\dot{R}_a$. Similarly, ϕ is here $\pm R_a\dot{R}_a$. Hence, the kinetic energy is $\pi\rho_L R_a^2\dot{R}_a^2 dy$, where dy is the lamina thickness. The root-mean-square velocity is then

$$u_b' = \left[\frac{2\pi R_a^2\dot{R}_a^2}{L^2 - \pi R_a^2}\right]^{\frac{1}{2}} = \dot{R}_a\left[\frac{2F}{1-F}\right]^{\frac{1}{2}} \sim \frac{2R_m}{\theta}\left[\frac{2F}{1-F}\right]^{\frac{1}{2}} \tag{30}$$

replacing the tangent by the chord. Note that Eq. (30) predicts the average liquid velocity to be

equal to the average bubble wall velocity, $2R_m/\theta$, when $L = \sqrt{3\pi/2}\, R_m$.

Consider now the case of K = 2, equivalent to the assumption that the time between bubbles for a given nucleation center is, on the average, equal to the bubble lifetime. Since half the nucleation centers are inactive at any given time, the situation may be represented by Fig. 7, where the crosses represent temporarily inactive sites, and every collapsing bubble (–) must be surrounded by growing bubbles (+) to maintain a constant fraction of the surface covered with bubbles. It can be seen that this case corresponds exactly to that in Fig. 6, except that now the diagonal of the unit cell L gives the distance between growing and collapsing bubbles.

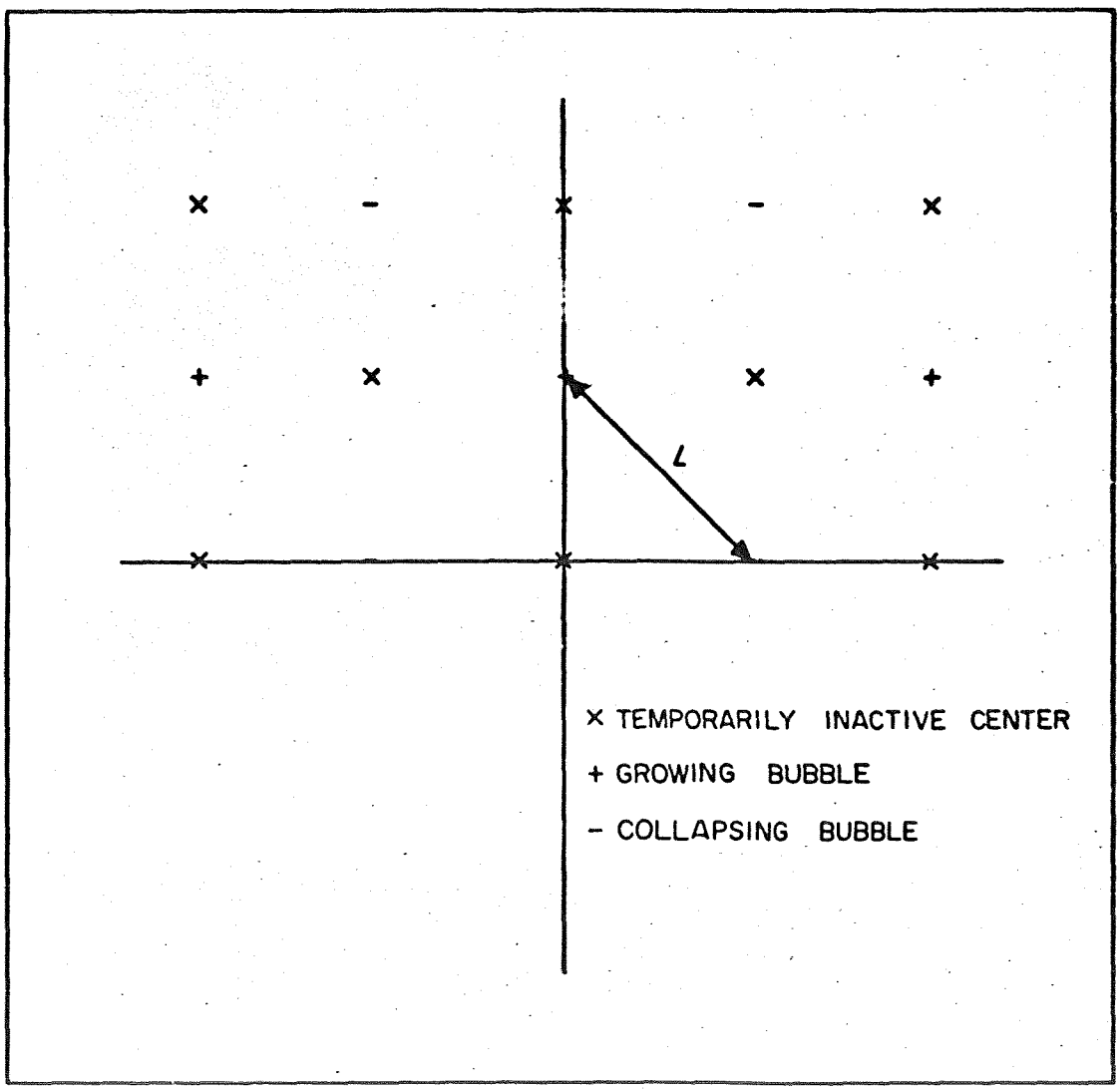

Fig. 7. Model of Assembly of Bubbles Growing and Collapsing on a Surface. Distance Between Centers L Large Compared with Mean Bubble Radius . ,. Staggered Net

Equation (30) applies equally well to this case. It requires only a slight extension of this reasoning to show that Eq. (30) describes the average liquid velocity induced by the bubbles parallel to the wall, independent of K.

Based on Eq. (30), the rms velocity induced by the bubbles u_b' is calculated in Table I and shown in Fig. 8 for the data of Gunther (Ref. 1), reproduced here as Figs. 9 through 11. These runs investigated the effect of liquid subcooling, liquid velocity and heat flux in a transparent flow channel 1/4 in. square in cross section divided by a heating strip 3/16-in. wide. The liquid was degassed, distilled water at slightly above atmospheric pressure. As expected, u_b' increases in each case as the upper limit of nucleate boiling is approached. The difficulty of obtaining accurate bubble counts is shown in Fig. 8, where u_b' calculated for supposedly identical conditions in Figs. 10 and 11 check within 10%, but between Figs. 9 and 11 check only within 50%.

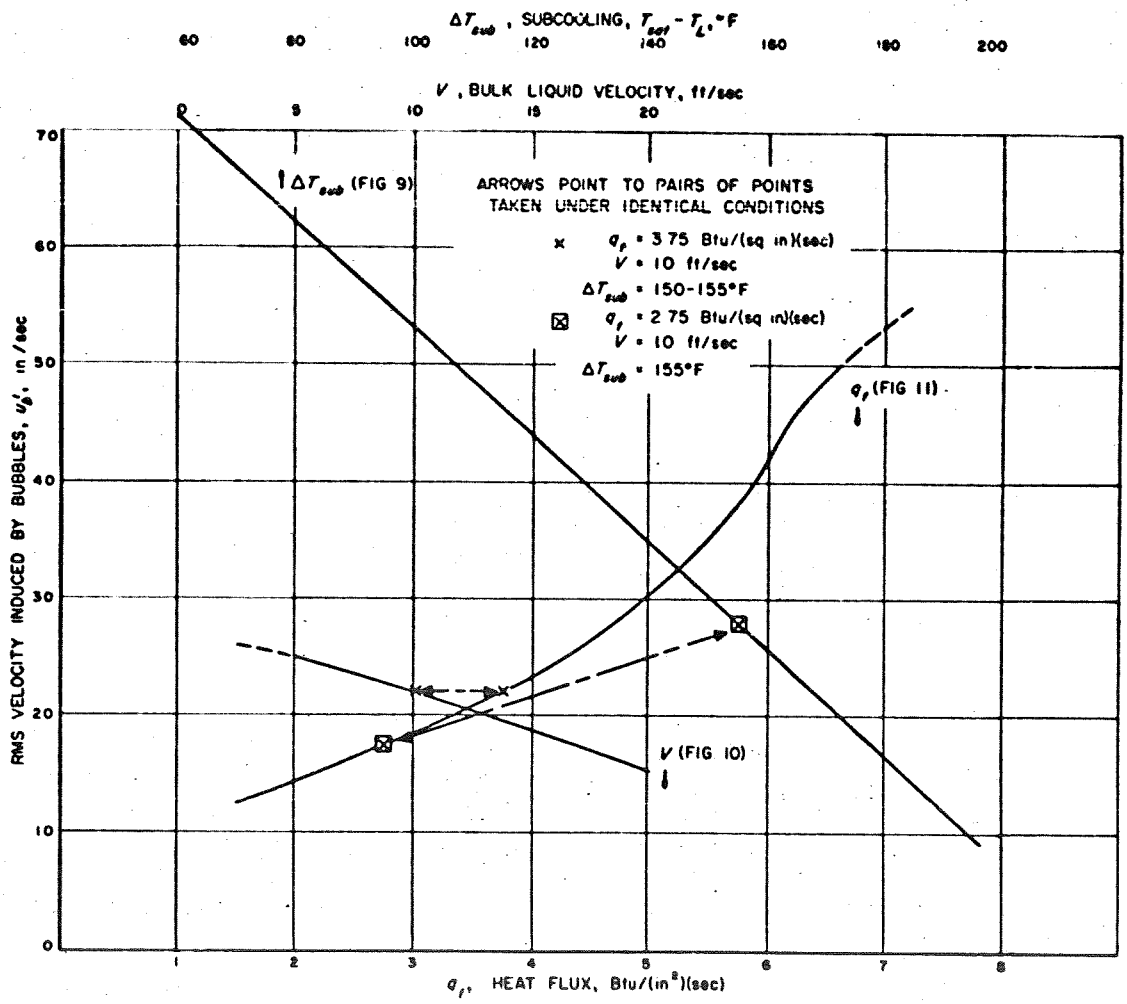

Fig. 8. RMS Velocity Induced by Bubbles in Gunther's Experiments (Figs. 8 through 10), Calculated by Eq. (30)

Table 1. Calculations of Bubble Parameters From Gunther's Data (Ref. 1)

V ft/sec	q/A Btu/(sq in.) (sec)	ΔT_{sub} °F	R_m in.	1 − F	$\alpha \times 10^6$ sec	u_b' [a] in./sec	$\frac{y_a}{y_1} - \frac{a}{R_m}$ [b]	$\frac{1}{C_H}$ [c]	$T_w - T_L$ °F	T_L °F	$T_1 - T_L$ [d] °F	T_1 °F
Group I [e]												
20	3.75	150	0.007	0.99	130	15.3	17.8	464	201	89	68.5	157.5
10	3.75	150	0.010	0.96	260	22.2	12.5	232	201	89	83	172
5	3.75	150	0.012	0.92	400	25.0	10.4	116	201	89	119.5	208.5
2.5	3.75	150	0.013	0.89	580	23.5	9.6	58	201	89	149.5	238.5
Group II [f]												
10	1.5	155	0.0115	0.99	250	12.5	10.9	584	199	84	48.5	132.5
10	2.5	155	0.011	0.98	250	17.8	11.4	350	202	84	65.5	149.5
10	3.5	155	0.0105	0.97	245	21.3	11.9	254	205	84	79.5	163.5
10	4.5	155	0.0095	0.955	220	26.5	13.2	200	207.5	84	94.5	178.5
10	5.5	155	0.0080	0.92	185	36.1	15.6	163.5	209	84	111.5	195.5
10	6.5	155	0.0065	0.84	150	53.5	19.2	140.5	211	84	131.5	215.5
10	7.5 [g,h]	155	0.005	0.65	115	99.0	25.0	122.5	212	34	154	238
Group III [i]												
10	2.75	60 [j]	0.020	0.62	605	73.4	6.2	169.5	107.5	179	37.5	216.5
10	2.75	100	0.017	0.825	410	54.0	7.4	232	147.5	139	48.5	187.5
10	2.75	140	0.013	0.94	270	34.4	9.6	295	187.5	99	61.5	160.5
10	2.75	160	0.010	0.97	215	23.1	12.5	326	207.5	79	72.5	151.5
10	2.75	180	0.007	0.98	175	16.2	17.8	357	227.5	59	86.9	146
10	2.75	200	0.0035	0.99	130	7.65	35.7	390	247.5	39	112	151

[a] Root-mean-square velocity induced by the bubbles, given by Eq. (30).

[b] Hydraulic radius, $a = 0.125$ in.

[c] Eq. (41).

[d] Eq. (42).

[e] Effect of velocity (Fig. 10). $q/A = 3.75$ Btu/(sq in.) (sec); $\Delta T_{sub} = 150$ F; $P = 50$ in. Hg.

[f] Effect of heat transfer rate (Fig. 11). $V = 10$ ft/sec; $\Delta T_{sub} = 155$ F; $P = 50$ in. Hg.

[g] Burnout.

[h] Extrapolated.

[i] Effect of subcooling (Fig. 9). $q/A = 2.75$ Btu/(sq in.) (sec); $V = 10$ ft/sec.

[j] Calculated from Ref. 7, assuming that T_w is a function only of the heat flux. Corrections for slight effect of pressure (50 in. Hg) made by assuming the excess vapor pressure (ΔP) due to the wall superheat to be constant over a small range of system pressure.

Blank

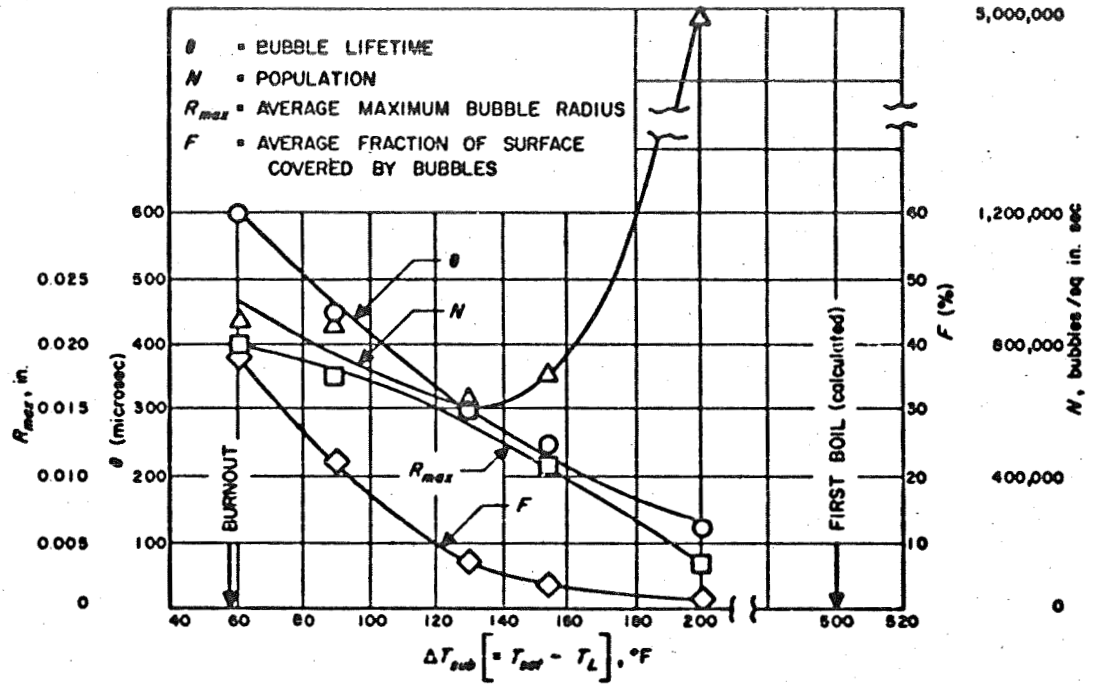

Fig. 9. Gunther's Data (Ref. 1 and Fig. 11): Effect of Subcooling

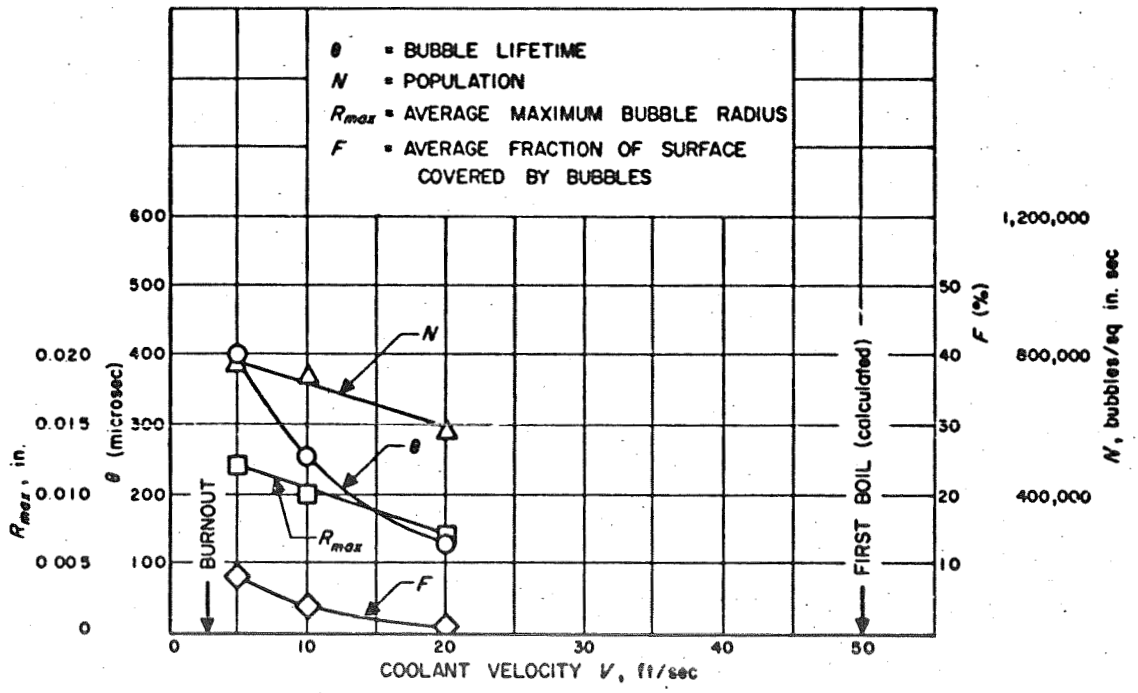

Fig. 10. Gunther's Data (Ref. 1 and Fig. 16): Effect of Velocity

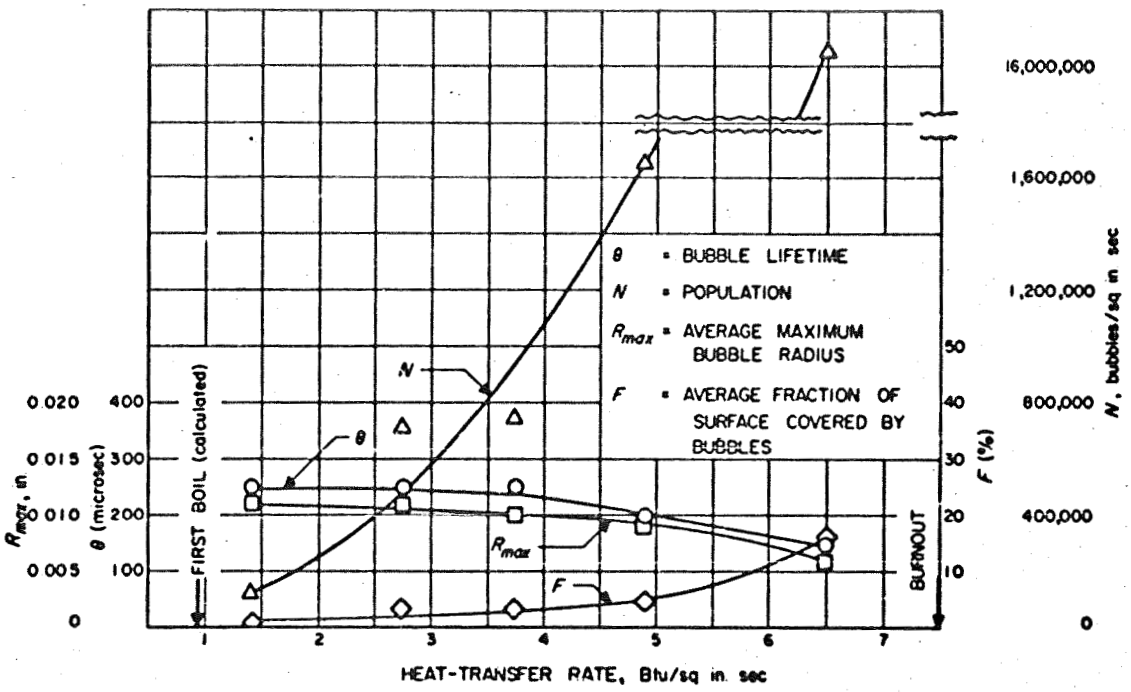

Fig. 11. Gunther's Data (Ref. 1 and Fig. 17): Effect of Heat Transfer Rate

V. SINGLE-PHASE TURBULENT CORE

At this point it is instructive to consider the temperature and velocity distributions in the single-phase turbulent core liquid, necessarily restricted here to subcooled boiling, since in saturated boiling the two-phase region extends throughout the tube.

Begin with the momentum equation, averaged with respect to time, for turbulent flow of a single-phase fluid in a tube:

$$\tau_t \left(1 - \frac{y}{a}\right) = -\rho_L \overline{u'v'} + \mu \frac{du}{dy} \tag{31}$$

where τ_t is the total shear stress at the wall, a is the pipe radius, and $\overline{u'v'}$ represents the time-averaged product of the velocity fluctuations in the x and y directions. Similarly, the energy equation is given by

$$q_t \left(1 - \frac{y}{a}\right) = -\rho_L C_L \overline{T'v'} + k_L \frac{dT}{dy} \tag{32}$$

where $\overline{T'v'}$ represents the time-averaged product of the fluctuations of the temperature and the velocity normal to the wall. The physical properties are here assumed constant, since, by the nature of nucleate boiling, the wall temperature is not far removed from the bulk liquid temperature. Also, the principal changes in the temperature and velocity profiles occur quite close to the wall, so that y/a can be neglected compared with unity. The usual assumption of the validity of the Reynolds analogy is made, so that

$$\frac{T'v'}{\frac{dT}{dy}} = \frac{1}{Pr_\tau} \frac{\overline{u'v'}}{\frac{du}{dy}} \tag{33}$$

Here Pr_τ is a turbulent Prandtl number, equivalent to the ratio of the eddy diffusivities for heat and momentum transfer and may be assumed to be unity for water and other nonmetallic liquids

(cf. Ref. 20). Also, the molecular shear-stress and heat-transfer terms are assumed to be negligible at distances far from the wall. With these assumptions it is possible directly to derive the well-established dimensionless equations (e.g., Refs. 20, 21, and 22) for the turbulent core:

$$u^+ - u_1^+ = \frac{1}{\kappa} \ln \frac{y^+}{y_1^+} \qquad y^+ > y_1^+ \tag{34}$$

and

$$u^+ - u_1^+ = T^+ - T_1^+ \qquad y^+ > y_1^+ \tag{35}$$

where

$$u^+ = \frac{u}{\sqrt{\frac{\tau_t}{\rho_L}}} \tag{36}$$

$$y^+ = \frac{y}{\nu} \sqrt{\frac{\tau_t}{\rho_L}} \tag{37}$$

$$T^+ = (T_w - T) \frac{\rho_L C_L}{q_t} \sqrt{\frac{\tau_t}{\rho_L}} \tag{38}$$

and κ is a universal constant which has been empirically determined to be about 0.4. The distance y_1 represents the dividing line between the turbulent core and the two-phase wall layer, and is of the order of R_m, the mean maximum bubble radius. It will be assumed that the mean velocity V and the mean temperature T_L occur at the same distance from the wall, y_a.

Now, some experimental evidence exists (Ref. 6) that Eq. (35) holds all the way to the wall in subcooled, forced-convection nucleate boiling systems, or

$$V^+ = T_L^+ \tag{39}$$

With this assumption it is possible to estimate the temperature T_1 at the edge of the turbulent core. Combining Eqs. (34), (35) and (39) gives

$$\frac{T_L^+ - T_1^+}{T_L^+} = \frac{T_1 - T_L}{T_w - T_L} = \frac{1}{\kappa V^+} \ln \left(\frac{y_a^+}{y_1^+} \right) \tag{40}$$

But since the Stanton number, C_H, is given by

$$\frac{1}{C_H} = \frac{(T_w - T_L)\, \rho_L C_L V}{q_t} = T_L^+ V^+ \tag{41}$$

Eqs. (39), (40), and (41) yield

$$\frac{T_1 - T_L}{T_w - T_L} = \frac{\sqrt{C_H}}{\kappa} \ln \frac{y_a}{y_1} \tag{42}$$

This equation may be applied to Gunther's data (Figs. 8 through 10) to estimate an approximate time-average liquid temperature at the edge of the two-phase wall layer. Assume that the mean temperature occurs at the centerline of the flow passage or at a distance corresponding to the hydraulic radius. Note that this assumption is not strictly correct, since the only heat input was from a thin stainless steel strip suspended along the centerline of the channel; but since the temperature in the turbulent core is relatively uniform, it is probably acceptable. With this assumption set $y_a = a$, the hydraulic radius, and $y_1 = R_m$ in Eq. (42). The wall temperature,

T_w, was calculated from Gunther and Kreith's surface temperature measurements (see Fig. 4 of Ref. 7), assuming that T_w at a given flux is independent of the liquid velocity and subcooling. A correction was made for the slight effect of pressure (50 in. Hg) on the wall superheat by assuming the vapor pressure difference corresponding to the wall superheat to remain constant over this small range of pressures. Essentially this is equivalent to assuming that the critical bubble radius, which is determined by the radius of the active nucleating cavities on the surface, remains constant. The calculated values of T_1 are shown in Table 1 and Fig. 11 as a function of liquid subcooling, liquid velocity, and heat flux. It is most interesting to note that in each series of runs T_1 rises steeply towards the saturation temperature (239°F) as burnout is approached. Thus, the maximum heat flux coincides with the appearance of a fairly thick layer of warm water next to the wall. This seems to indicate that at conditions far removed from burnout the principal resistance to heat transfer is in the two-phase wall layer; but as the flux is increased, or the bulk velocity reduced, or the subcooling decreased, the resistance of the turbulent core becomes appreciable. (See Fig. 12) Burnout occurs when the core is unable to remove the heat as fast as it can be transmitted by the wall layer ($q_c^{(2)}$ in Eq. (7)), resulting in a marked increase in bubble size and population, which in turn results in bubble coalescence.

Support for this concept is found in Gunther's (Ref. 1) empirical correlation of the maximum heat flux with liquid velocity and temperature:

$$\left(\frac{q}{A}\right)_{burnout} = 0.0135\, V^{0.5}\, \Delta T_{sub} \qquad (43)$$

The form of this equation strongly suggests that the maximum heat flux is equal to the product of a turbulent heat-transfer coefficient, which is proportional to the liquid velocity to a power between 0.5 and 0.8 and the mean temperature difference between the saturation temperature, characteristic of the liquid near the top of the bubbles, and the bulk liquid. From this point of view, the two-phase wall layer at maximum heat flux acts as a completely rough wall, and the transfer of heat from this rough wall is proportional to the product of a turbulent heat transfer coefficient and a temperature driving force. At constant bulk liquid velocity and subcooling, the "roughness" of the wall adjusts itself to the heat flux; but at burnout the increase in "roughness" can no longer match the increase in heat flux.

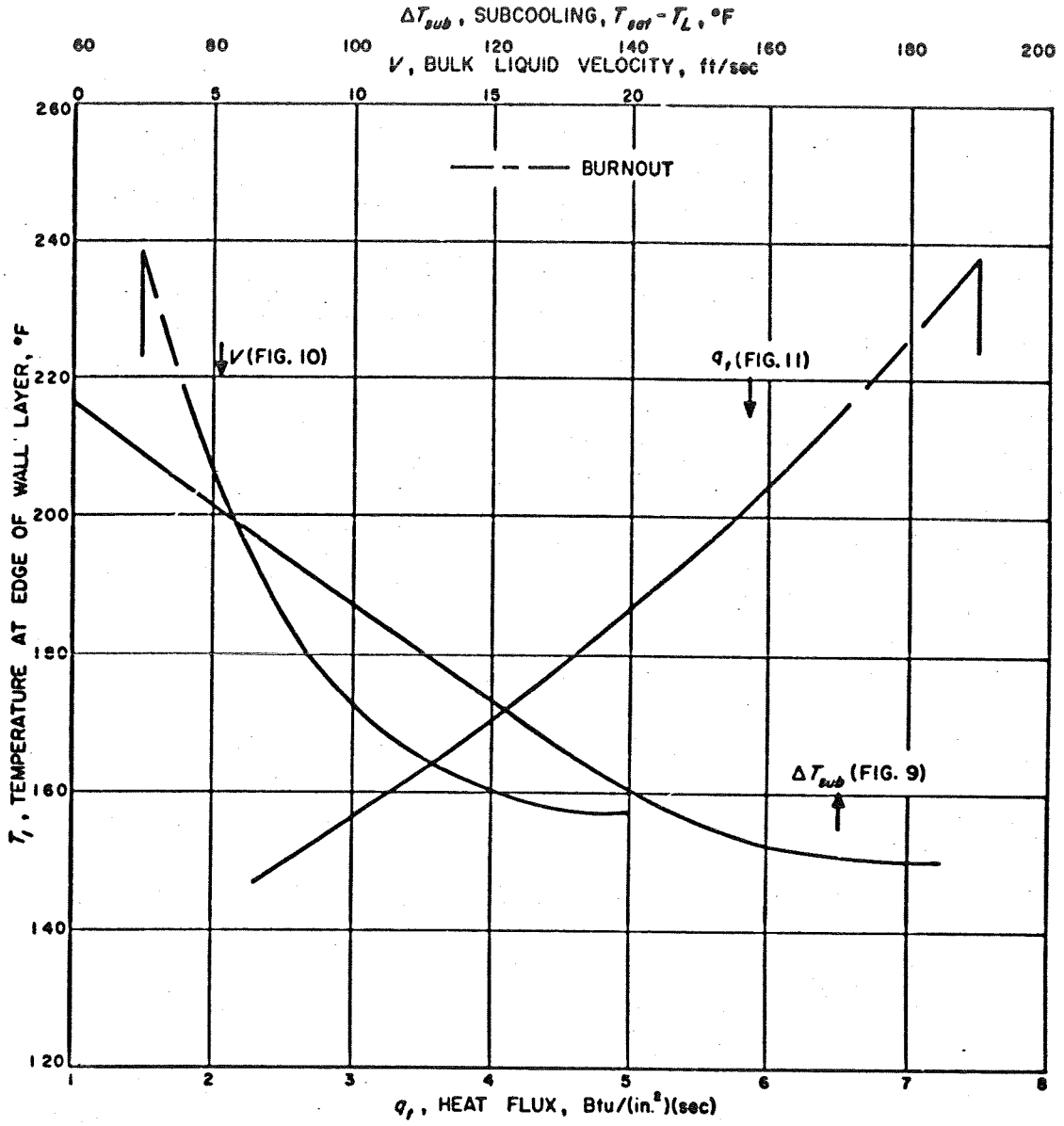

Fig. 12. Temperature at Edge of Two-Phase Layer in Gunther's Experiments (Figs. 9 through 11), Calculated by Eq. (42)

VI. HEAT FLOW THROUGH THE TWO-PHASE WALL LAYER

A. Inner Layer Heat Flow

It is now possible to formulate some rather speculative expressions for the heat flow in the first and third steps of the three-step model proposed in Sec. II. The second step is not considered here, in view of the uncertainty concerning the magnitude of latent heat transport. For the first step, the heat flow from the wall to the adjacent liquid is given by Eq. (4). The quenching heat flux, q_q, is given by Eq. (25). Proceed now to calculate the stirring heat flux, q_{bc}, assuming a form similar to Eq. (32):

$$q_w = \left(- \rho_L C_L \overline{T'v'} + k_L \frac{dT}{dy} \right)(1 - f) \tag{44}$$

where

$$f \cong 2KF \tag{45}$$

It may be noted that $(1 - 2KF)$ is the approximate fraction of the heating surface which is not periodically covered by bubbles. The temperature fluctuation T' and the velocity fluctuation v' are made up of components due to the bubbles and to the diffusion of turbulence from the bulk stream. For the purposes of our simple analysis, however, it will be assumed that turbulent eddies diffusing towards the wall from the main stream are considerably weaker very near the wall than the eddies produced by the bubbles themselves. This is reasonable, in view of the intense microconvection adjacent to the wall induced by the growing and collapsing bubbles. Further, it is assumed that the molecular heat conduction term rapidly becomes negligible a short distance from the wall, so that Eq. (44) becomes

$$q_w = - \rho_L C_L \overline{T_b' v_b'} (1 - 2KF) \tag{46}$$

It is now necessary to fall back upon a dimensional approach, in which the time-average product

in Eq. (46) is assumed to be proportional to the product of a characteristic velocity and a characteristic temperature difference. The natural choice is

$$\overline{T_b' v_b'} = \beta_1 u_b' (T_w - T_L) \tag{47}$$

where u_b' is descriptive of the mean velocity fluctuation due to the bubbles, $T_w - T_L$ is descriptive of the temperature driving force, and β_1 is an empirical constant.

Combining Eqs. (25), (44), (46), and (47) gives the following expression for the total heat flux:

$$q_t = q_q + q_w = 5.01\, N (T_w - T_1) R_m^2 \sqrt{\rho_L C_L k_L \theta}\, \psi(\mathrm{K}) \left(1 + \frac{0.4 V \theta}{R_m}\right)$$

$$+ \beta_1 \rho_L C_L u_b' (T_w - T_L)(1 - 2KF) \tag{48}$$

It is of interest to see whether this expression can be fitted to Gunther's data by an appropriate choice of β_1, the empirical proportionality constant. For our simple calculation, assume that K, the ratio of the bubble period to the bubble lifetime, is 1.5, since a bubble frequency of about 1000 cps and a bubble lifetime of 6.4×10^{-4} sec have been reported (Ref. 7) in subcooled pool boiling (q_t = 2.0 Btu/(sq in.) (sec); T_L = 98°F). The calculations of the quenching heat flux are given in Table 2; with the choice β_1 = 0.025 to give the best fit, reasonably good agreement is obtained with Gunther's smoothed data (Table 3 and Figs. 13 and 14). The data investigating the effect of bulk liquid subcooling are not included, since at moderate subcoolings some of the bubbles detach from the wall, with the result that the extent of the two-phase wall layer becomes uncertain.

Referring to Figs. 13 and 14, it is seen that a reasonably good fit exists between the predicted and the experimental total heat flux. Of interest are the following points:

1. The quenching heat flux, q_q, is appreciable but is less than the convective flux q_w, except at high bubble populations, where the fraction of the surface which is never covered by bubbles becomes quite small (Table 3).

2. In both cases, the predicted q_t falls below the experimental q_t close to the burnout point. This is partly because f, the fraction of the surface which is in occasional contact with bubbles, increases sharply (and hence q_w decreases) as burnout is approached; and partly because T_1 rises rapidly near the burnout point, as noted previously, so that the quenching heat flux does not increase at the same rate as does $(f - F)$, the fraction of the surface being quenched at any instant (cf. Sec. IV). This is to say that the bare spots are quenched with warmer liquid as burnout is approached.

3. The predicted total flux is low at high stream velocities and relatively small ($F < 0.02$) bubble populations (Figs. 10 and 13). This might be expected, from the neglect of the stream-induced turbulence in Eq. (48).

B. Outer Layer Heat Flow

Similarly, expressions for the third step of the heat flow model, Eq. (7), from the edge of the two-phase wall layer into the turbulent core, can be speculatively constructed.

To begin with, it will be assumed that the equations for the turbulent core (Eqs. 31, 32, and 33) are also valid at the edge of the two-phase wall layer. The problem then resolves itself into determining the increased drag due to the bubbles. In the outer portion of the two-phase wall layer, which is assumed to be thin compared with the hydraulic radius, Eq. (32) becomes, upon neglecting molecular conduction

$$q_t = -\rho_L C_L \overline{T'v'} = -\rho_L C_L \overline{(T_b' + T_s')(v_b' + v_s')} \tag{49}$$

where T_b' and T_s' are the temperature fluctuations due to the bubble and the stream motion, and v_b' and v_s' are the corresponding velocity fluctuations normal to the wall. Actually, there is undoubtedly an interaction between the bubbles and the turbulent core; but for this simple analysis it will be assumed that the time-average product in (Eq. 49) can be decomposed into the sum of two time-average terms:

$$\overline{(T_b' + T_s')(v_b' + v_s')} = \overline{T_b' v_b'} + \overline{T_s' v_s'} \tag{50}$$

Table 2. Calculation of Quenching Heat Flux From Gunther's Data (Ref. 1)

V ft/sec	q/A Btu/(sq in.) (sec)	ΔT_{sub} °F	$N \times 10^{-5}$ Bubbles/ (sq in.) (sec)	$T_w - T_1$ °F	$5.01 N(T_w - T_1)$ °F/(in.)^2 (sec)	$R_m^2(\rho_L C_L k_L \theta)^{1/2}$ Btu/°F	$1 + \frac{0.4 V\theta}{R_m}$	$q_{q'}$ Btu/(sq in.) (sec) [a] K = 1.5	K = 2	K = 3
Group I [b]										
20	3.75	150	6.0	132.5	3.98×10^{-8}	3.07×10^{-9}	2.78	0.21	0.27	0.36
10	3.75	150	7.3	118	4.32	8.85	2.25	0.52	0.68	0.91
5	3.75	150	7.8	81.5	3.19	15.8	1.80	0.55	0.71	0.96
2.5	3.75	150	8.0	51.5	2.06	21.1	1.48	0.39	0.51	0.68
Group II										
10	2.5	155	4.0	136.5	2.74×10^{-8}	11.5×10^{-9}	2.04	0.39	0.51	0.68
10	3.5	155	8.1	125.5	5.09	10.4	2.12	0.68	0.88	1.19
10	4.5	155	14.0	113	7.92	8.98	1.97	0.85	1.10	1.48
10	5.5	155	37	97.5	18.5	5.83	2.11	1.38	1.79	2.41
10	6.5	155	160.5	79.5	64.0	2.84	1.96	2.15	2.80	3.78
10	7.5	155	542	58	156.5	1.47	1.96	2.72	3.54	4.78
Group III										
10	2.75	60	9.4	70	3.29×10^{8}	54.0×10^{-9}	2.26	2.43	3.16	4.27
10	2.75	100	7.2	99	3.57	32.1	2.01	1.40	1.82	2.45
10	2.75	140	6.2	126	3.91	15.2	1.87	0.68	0.88	1.18
10	2.75	160	7.3	135	4.94	8.98	2.03	0.52	0.67	0.91
10	2.75	180	14	140.5	9.86	3.63	2.20	0.48	0.62	0.83
10	2.75	200	57	135.5	38.7	0.767	2.55	0.46	0.60	0.80

[a] Eq. (25). ψ (K) calculated from Eq. (22) (Fig. 4).

[b] See Table 1 and Figs. 9, 10, and 11.

Blank

Table 3. Calculation of Heat Flow From Gunther's Data (Ref. 1)

V ft/sec	q/A Btu/(sq in.) (sec)	$u_b'(1-3F)(T_w-T_L)$ (in.)(°F)/sec	q_q [a] Btu/(sq in.) (sec)	q_w [b] Btu/(sq in.) (sec)	$q_f = q_w + q_q$ [c] Btu/(sq in.) (sec)	$q_s^{(2)}$ [d] Btu/(sq in.) (sec)	Re	$\left(\frac{F}{1-F}\right)$	$\frac{T_w - T_L}{V}$ (°F)(sec)/ft	$u_b'^2 \times 10^{-2}$ $in.^2/sec^2$	$\left(\frac{F}{1-F}\right)^{0.425}$	$q_{bc}^{(2)}$ [e] Btu/(sq in.) (sec)	$q_s = q_{bc}^{(2)} + q_s^{(2)}$
Group I [f]													
20	3.75	2.89×10^3	0.21	2.39	2.60	3.31	49,800	0.0101	10.1	2.31	0.143	0.65	3.96
10	3.75	3.83	0.52	3.16	3.68	1.90	24,900	0.0417	20.1	4.96	0.260	1.54	3.44
5	3.75	3.73	0.55	3.08	3.63	1.09	12,450	0.0870	40.2	6.25	0.355	2.83	3.92
2.5	3.75	3.65	0.39	3.02	3.41	0.63	[f] 6,220	0.124	80.4	7.71	0.413	6.01	6.64
Group II													
10	2.5	3.17	0.39	2.62	3.01	1.85	23,500	0.0204	20.2	3.06	0.193	1.28	3.03
10	3.5	3.83	0.68	3.17	3.85	1.91	23,500	0.0309	20.5	4.56	0.229	1.63	3.54
10	4.5	4.56	0.85	3.78	4.63	1.96	23,500	0.0472	20.7	6.97	0.275	2.11	4.07
10	5.5	5.57	1.38	4.61	5.99	2.01	23,500	0.0870	20.9	13.0	0.355	3.08	5.09
10	6.5	5.26	2.15	4.35	6.50	2.04	23,500	0.191	21.1	24.5	0.495	4.18	6.22
10	7.5	-	2.72	-	2.72	2.04	23,500	0.539	21.2	47.9	0.770	5.30	7.34

[a] K, the ratio of the bubble period to bubble lifetime, taken to be 1.5. See Table 2.

[b] Eq. (48). β_1 chosen to give best fit; $\beta_1 = 0.023$.

[c] Eq. (48).

[d] Eq. (58). $Re = DV_s/\mu_L$; $D = 0.25$ in.

[e] Eq. (57). $\beta_3 = 0.575$.

[f] See Table 1 and Figs. 10 and 11.

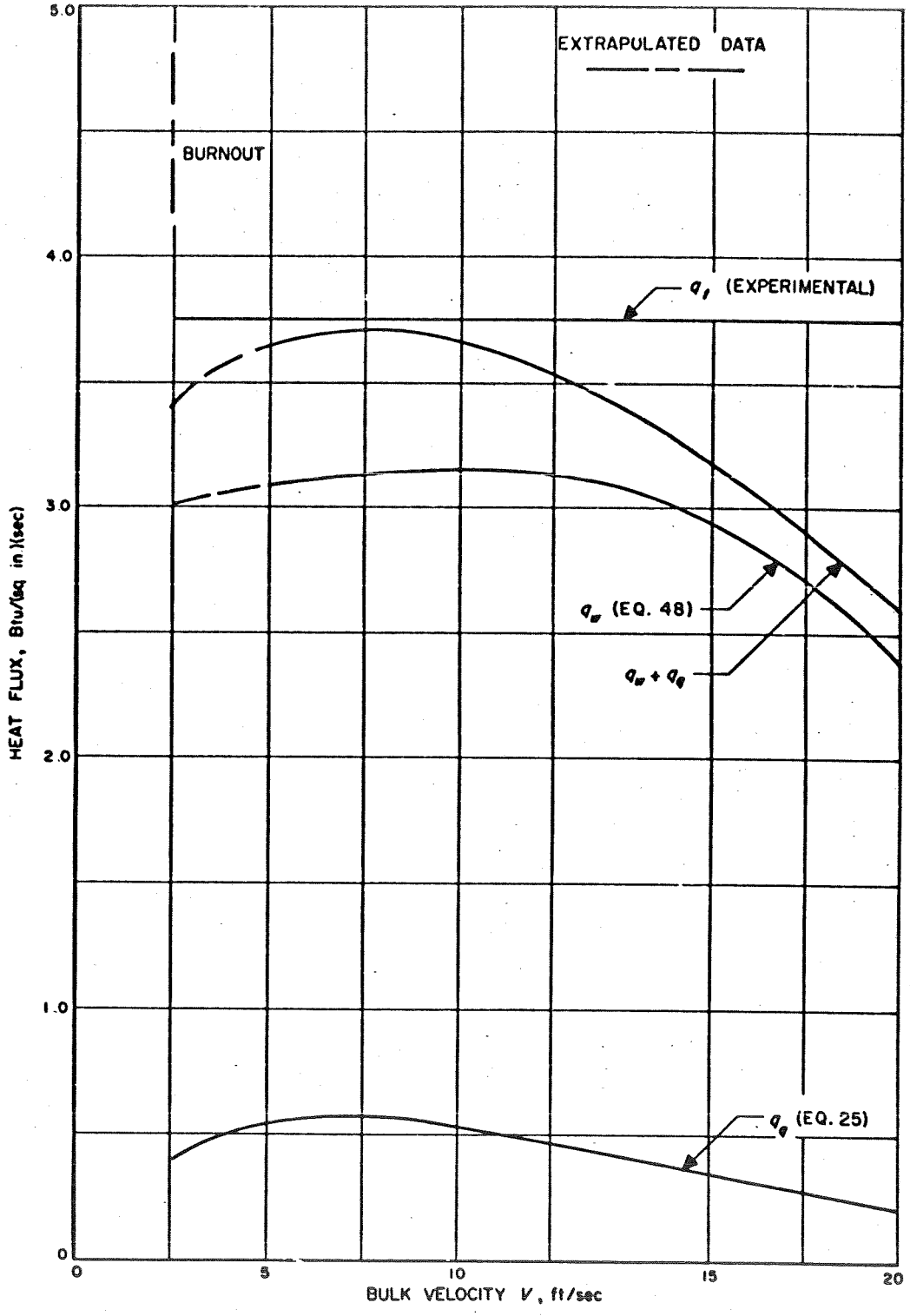

Fig. 13. Inner Layer Model Calculated for Gunther's Data (Fig. 10)

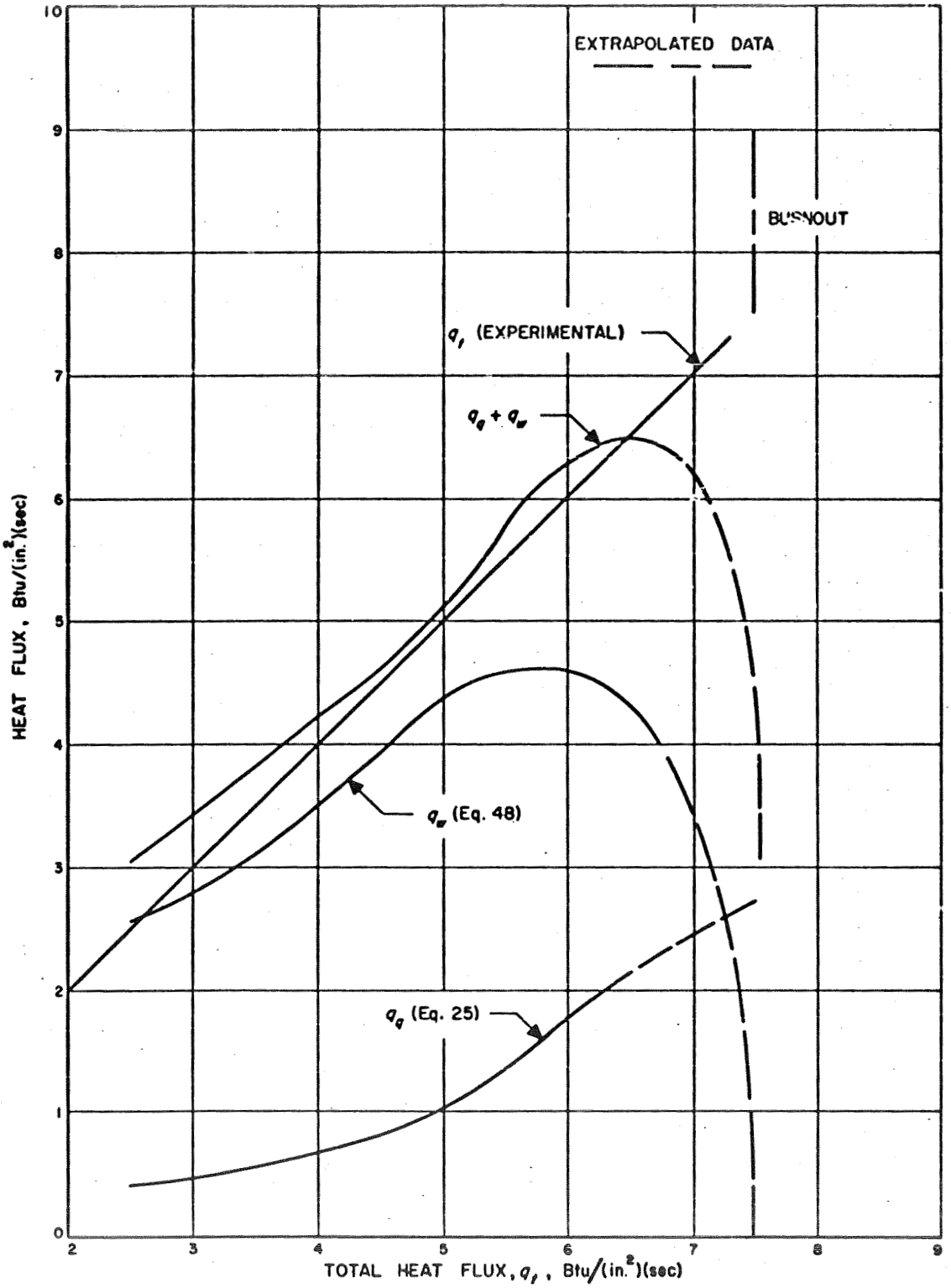

Fig. 14. Inner Layer Model Calculated for Gunther's Data (Fig. 11)

or

$$q_t^{(2)} = q_{bc}^{(2)} + q_s^{(2)} = -\rho_L C_L (\overline{T_b' v_b'} + \overline{T_s' v_s'}) \tag{51}$$

where $q_{bc}^{(2)}$ and $q_s^{(2)}$ are the heat fluxes due to the stirring action of the bubbles and of the stream, respectively. The analogy to the hypothesis of Rohsenow and Clark (Ref. 8) that the heat flux in convective boiling systems is the sum of the nonboiling convective heat flux, plus the pool boiling heat flux at the same surface temperature, may be noted. It will be assumed that $q_s^{(2)}$ is the nonboiling convective heat flux in the same system. Substituting Eq. (33), and assuming the eddy diffusivities for momentum and heat transfer to be equal,

$$q_t = q_s^{(2)} + \rho_L C_L (\overline{u_b' v_b'}) \left(\frac{dT}{du}\right) \tag{52}$$

From Eqs. (35) and (39),

$$\frac{dT}{du} \simeq \frac{T_w - T_L}{V} \tag{53}$$

It remains to choose an appropriate expression for $\overline{u_b' v_b'}$. If the heat transfer occurs entirely at the tops of the bubbles (latent heat transport), one would expect the mean bubble wall velocity to be applicable:

$$\overline{u_b' v_b'} \sim \left(\frac{R_m}{\theta}\right)^2 \tag{54}$$

If, however, the heat transfer between bubbles is the major factor, one would expect the mean velocity induced by the bubbles to be more appropriate:

$$\overline{u_b' v_b'} \sim u_b'^2 = 8 \left(\frac{R_m}{\theta}\right)^2 \left(\frac{F}{1-F}\right) \tag{55}$$

Hence, set

$$\overline{u_b' v_b'} = \beta_2 \left(\frac{R_m}{\theta}\right)^2 \left(\frac{F}{1-F}\right)^{\beta_3} \qquad 0 < \beta_3 < 1 \tag{56}$$

where β_2 and β_3 are empirical constants. Combining (52), (53), and (56),

$$q_t = q_{bc}^{(2)} + q_s^{(2)} = q_s^{(2)} + \beta_2 \rho_L C_L \left(\frac{T_w - T_L}{V}\right) \left(\frac{R_m}{\theta}\right)^2 \left(\frac{F}{1-F}\right)^{\beta_3} \tag{57}$$

The nonboiling flux is determined from a standard correlation such as the Sieder-Tate equation:

$$\frac{q_s^{(2)}}{\rho_L C_L V (T_w - T_L)} = \frac{0.023 \left(\frac{\mu_L}{\mu_w}\right)^{0.14}}{(Pr)^{\frac{2}{3}} (Re)^{0.2}} \tag{58}$$

where μ_L and μ_w are the viscosities evaluated at T_L and T_w, and the Reynolds number is based on the tube diameter and the mean bulk liquid velocity.

Once again, values of the empirical constants ($\beta_2 = 0.083$; $\beta_3 = 0.575$) were chosen in an attempt to fit Gunther's smoothed data (Figs. 10 and 11). The results are calculated in Table 3 and presented in Figs. 15 and 16. It is seen that there is reasonably close agreement between the experimental and the predicted total heat fluxes.

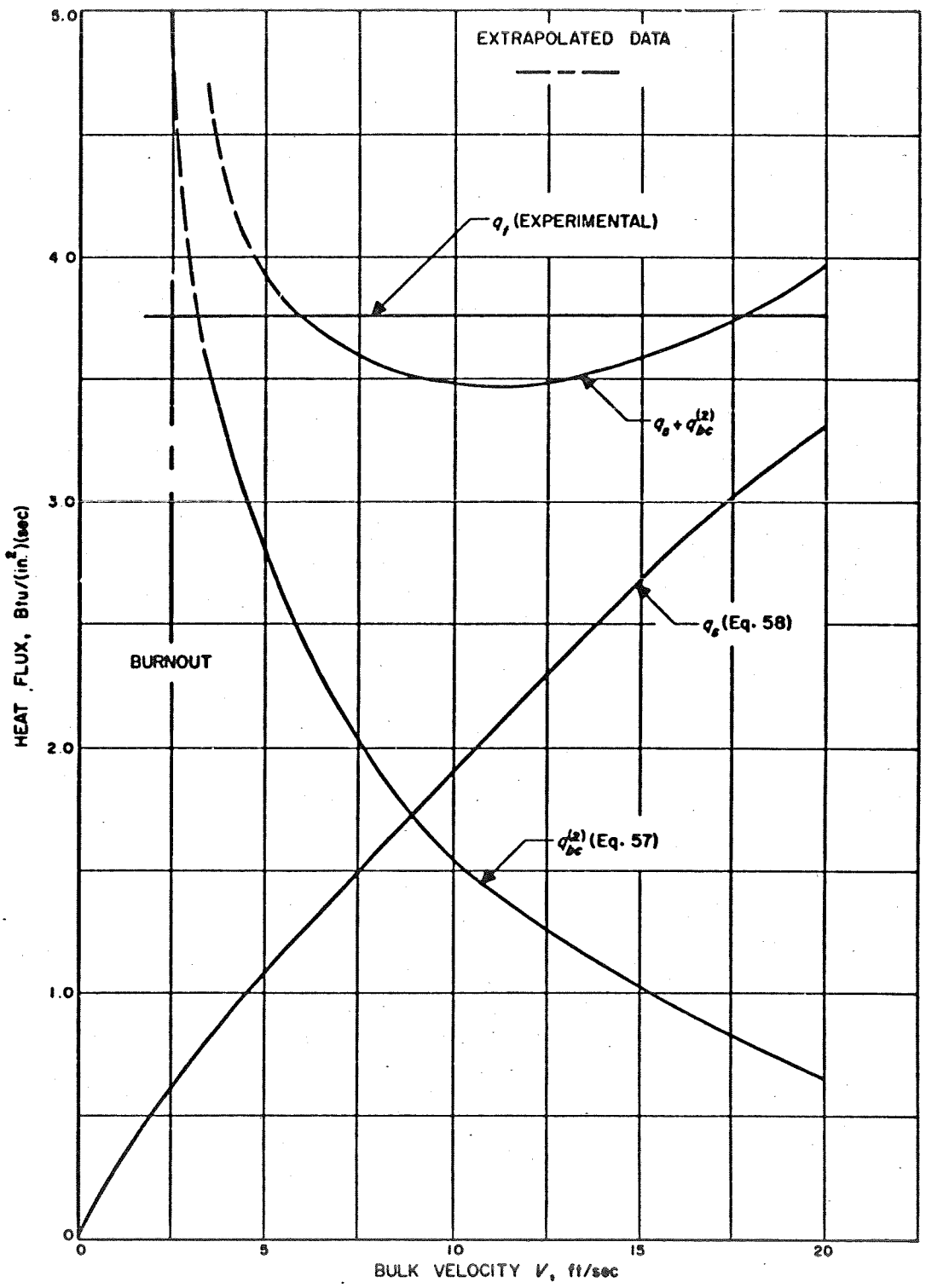

Fig. 15. Outer Layer Model Calculated for Gunther's Data (Fig. 10)

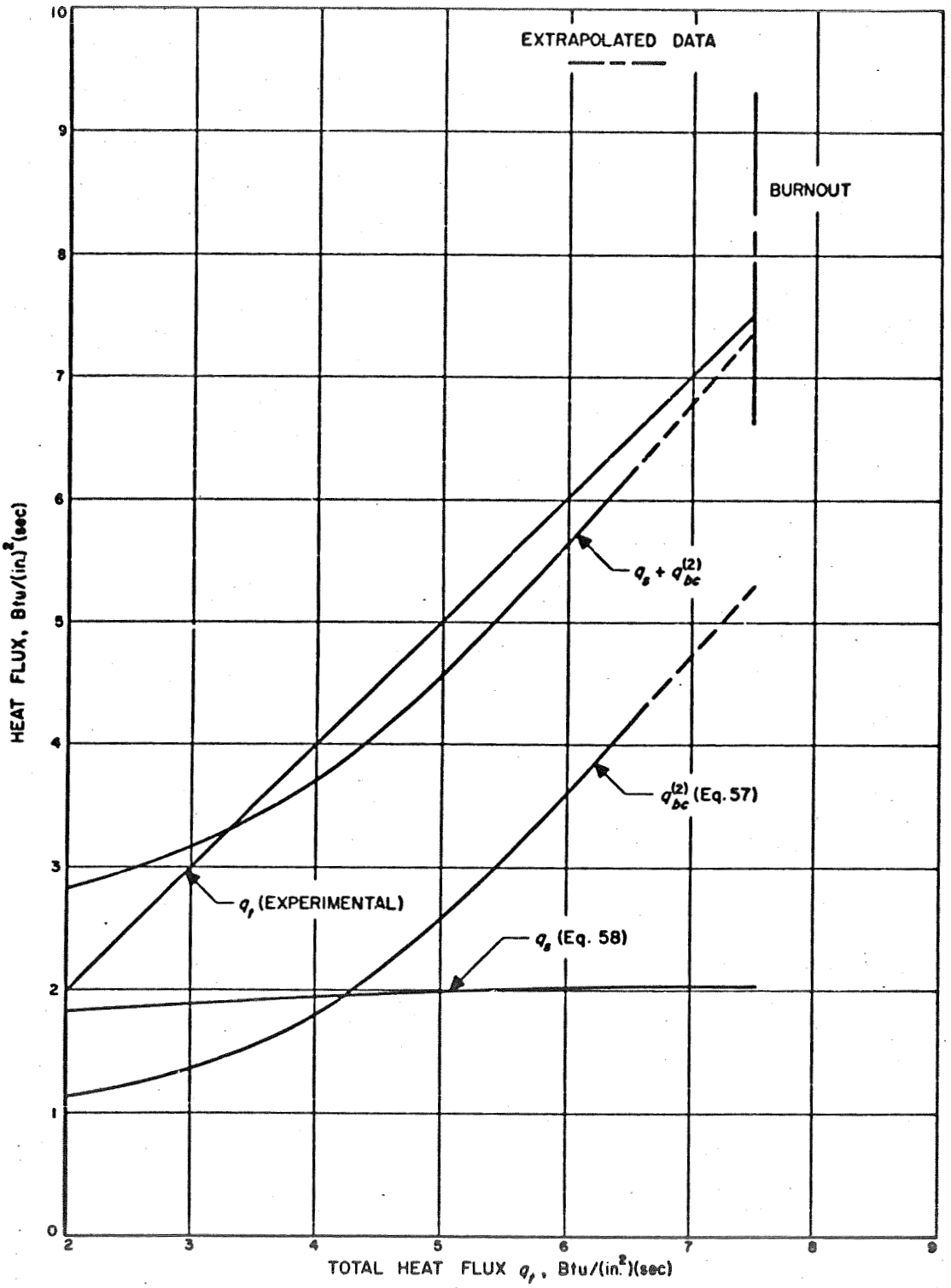

Fig. 16. Outer Layer Model Calculated for Gunther's Data (Fig. 11)

VII. DISCUSSION AND SUMMARY

The heat flow expressions derived in the preceding section are highly speculative, in view of the many simplifying assumptions. Considerably more data are required before they can be put on a firm footing. On the other hand, the three-step model proposed in Sec. II is not considered to be speculative; it is, in fact, a simple statement of the physical situation in highly subcooled nucleate boiling. In two previous papers (Refs. 9 and 10) turbulent convection was shown probably to control in the removal of heat from the bubble condensing surface; further evidence is adduced in Sec. III that latent heat transport is not negligible in comparison with the convective heat flow through the liquid between the bubbles. It is interesting (and perhaps coincidental) that the variation in maximum heat flux with pressure in saturated pool boiling can be reasonably well fitted by an expression based on latent heat transport. It is similarly interesting (and physically reasonable) that the temperature at the edge of the two-phase wall layer in highly subcooled nucleate boiling rises sharply towards the saturation temperature as burnout is approached. When the bubbles no longer grow into a zone of cold liquid, one may expect their size and number to increase rapidly and an instability to set in. Experimental measurements of the local bubble parameters in nucleate boiling are sorely needed. Such measurements are, in some cases, quite difficult; but a great deal could be learned from temperature and velocity information taken in simplified systems, such as one, two, or three bubbles growing and collapsing on a surface.

ACKNOWLEDGMENT

The major portion of this work was done at Rose Polytechnic Institute under a grant from the National Science Foundation. Ernest R. Davidson and Glenn A. Miles assisted in the calculations.

NOMENCLATURE

a = hydraulic radius of tube.

B = parameter defined by Eq. (23).

b = parameter defined by Eq. (23).

C_H = Stanton number.

$$= \frac{q_t}{\rho_t C_L V(T_w - T_L)}$$

C_L = specific heat of liquid.

F = time-average fraction of surface covered by bubbles.

f = fraction of surface periodically covered by bubbles.

H = enthalpy increase of liquid due to heat conduction upon collapse of one bubble.

$\vec{t}$ = unit vector parallel to the wall.

k_L = thermal conductivity of liquid.

k = modulus of elliptic function (Appendix A).

k' = quarter period of elliptic function (Appendix A).

K = parameter defined by Eq. (17).

L = distance between adjacent nucleation centers.

m = strength of spherical source of velocity potential.

m' = strength of line source of velocity potential.

n = normal to boundary (Eq. 29).

N = number of bubbles per unit wall area per unit time.

p = pressure.

Pr = Prandtl number of liquid.

Pr_t = turbulent Prandtl number (Eq. 45).

q_b = heat flux from surface beneath bubbles.

NOMENCLATURE (Cont'd.)

q_{bc} = heat flux due to stirring of bubbles (Eq. 49).

q_c = heat flux from surfaces between bubbles.

$q_s^{(2)}$ = heat flux due to stirring of stream (Eq. 51).

q_q = quenching heat flux.

q_t = total heat flux.

$q_b^{(1)}$ = latent heat flux.

q_u = heat flux from portion of surface periodically covered by bubbles.

q_w = heat flux from portion of surface which is not periodically covered by bubbles.

R = bubble radius.

R_m = maximum bubble radius.

Re = stream Reynolds number.

$\dot{R}_a$ = average bubble wall velocity.

r = radial distance.

s = parameter defined by (Eq. 17).

S = surface.

t = time.

T = temperature.

T' = fluctuation in temperature.

T^+ = dimensionless temperature, defined by Eq. (38).

T_0 = mean temperature of bubble evaporative surface.

T_1 = mean temperature at the edge of the two-phase wall layer.

T_2 = mean temperature of bubble condensing surface.

T_L = mean bulk liquid temperature.

T_{sat} = saturation temperature.

NOMENCLATURE (Cont'd.)

T_w = wall temperature.

V = mean stream velocity.

v' = fluctuation in velocity perpendicular to wall.

u = velocity parallel to the wall.

u' = fluctuation in velocity parallel to wall.

u_b' = root-mean-square velocity parallel to the wall induced by bubbles, defined by Eq. (30).

u^+ = dimensionless velocity, defined by Eq. (36).

w = complex velocity potential.

x = distance parallel to wall.

y = distance from wall.

y_1 = thickness of two-phase wall layer ($\sim R_m$).

y^+ = dimensionless distance, defined by Eq. (37).

z = complex position variable.

α = thermal diffusivity of liquid.

$\beta_1, \beta_2, \beta_3$ = empirical constants.

ϵ = accommodation coefficient for evaporation or condensation.

η = volume of liquid.

ζ = parameter defined by Eq. (17).

κ = universal velocity distribution constant, Eq. (34).

θ = bubble lifetime.

θ' = bubble period from a given nucleation center.

λ = latent heat of vaporization.

μ_L = viscosity of liquid evaluated at bulk temperature.

μ_w = viscosity of liquid evaluated at wall temperature.

NOMENCLATURE (Cont'd.)

ν = kinematic viscosity.

ξ = parameter defined by Eq. (23).

ρ_L = density.

τ = shear stress.

ϕ = velocity potential.

$\psi(K)$ = function defined by Eq. (46).

ω = function defined by Eq. (A-3) or (A-5).

∇ = gradient operator.

Superscripts

$\rightarrow$ = vector quantity.

$\overline{(\,)}$ = time average.

$(\,)'$ = fluctuation (unless otherwise defined).

$+$ = dimensionless quantity.

$\dot{(\,)}$ = derivative with respect to time.

(1) = heat flow from inner to outer portion of wall layer.

(2) = heat flow from outer portion of wall layer to turbulent core.

$(\,)^*$ = heat flow calculated on basis of actual heat transfer surface. Absence of star denotes heat transfer calculated on basis of total wall area.

Subscripts

a = average.

b = bubble.

NOMENCLATURE (Cont'd.)

bc = convection due to bubbles.

c = convection.

L = bulk liquid.

m = maximum.

q = quenching.

s = stream.

sat = saturation.

t = total.

u = unwetted.

v = vapor.

W = wall.

w = wetted.

1 = edge of two-phase wall layer.

REFERENCES

1. Gunther, Fred C., *Photographic Study of Surface-Boiling Heat Transfer to Water with Forced Convection*, Progress Report No. 4-75. Pasadena: Jet Propulsion Laboratory, June 28, 1950.

2. Batchelor, G. K., *The Theory of Homogeneous Turbulence*. Cambridge: Cambridge University Press, 1953.

3. Cramer, H., *Mathematical Methods of Statistics*. Princeton: Princeton University Press, 1946.

4. Frenkel, J., *Kinetic Theory of Liquids*, p. 329. New York: Dover Publications, Inc., 1935.

5. Bankoff, S. G., Colahan, W. J., Jr., and Bartz, D. R., *Summary of Conference on Bubble Dynamics and Boiling Heat Transfer at the Jet Propulsion Laboratory, June 14 and 15, 1956*, Memorandum No. 20-137. Pasadena: Jet Propulsion Laboratory, December 10, 1956.

6. Sabersky, R. H., and Mulligan, H. E., "On the Relationship Between Fluid Friction and Heat Transfer in Nucleate Boiling," *Jet Propulsion*, 25 (No. 1): 9-12, January, 1955.

7. Gunther, F. C., and Kreith, F., *Photographic Study of Bubble Formation in Heat Transfer in Subcooled Water*, Progress Report No. 4-120. Pasadena: Jet Propulsion Laboratory, March 9, 1950.

8. Rohsenow, W. M., and Clark, J. A., "A Study of the Mechanism of Boiling Heat Transfer," *Transactions of the American Society of Mechanical Engineers*, 73: 609-620, July, 1951.

9. Bankoff, S. G., and Mikesell, R. D., "Bubble Growth Rates in Highly Subcooled Nucleate Boiling" (to be published).

10. Bankoff, S. G., and Mikesell, R. D., "Growth of Bubbles in a Liquid of Initially Non-Uniform Temperature" (to be published).

11. Plesset, M. S., and Zwick, S. A., "Stability of Fluid Flows with Spherical Symmetry," *Journal of Applied Physics*, 25: 493-500 (1954).

12. Ellion, M. E., *A Study of the Mechanism of Boiling Heat Transfer*, Memorandum No. 20-88. Pasadena: Jet Propulsion Laboratory, March, 1954.

13. McAdams, W. H., *Heat Transmission*. New York: McGraw-Hill Book Company, 1954.

14. Cichelli, M. T., and Bonilla, C. F., "Heat Transfer to Liquids Boiling Under Pressure," *Transactions of the American Institute of Chemical Engineers*, 41: 755-787, 1945.

REFERENCES (Cont'd)

15. Plesset, M. S., "Note on the Flow of Vapor Between Liquid Surfaces," *Journal of Chemical Physics*, 20 (No. 5): 790-793, 1952.

16. Roald, B., and Beck, W., "Dissolution of Magnesium in Hydrochloric Acid," *Journal of the Electrochemical Society*, 98 (No. 7): 227-290, 1951.

17. Jakob, M., *Heat Transfer*, vol. I. New York: John Wiley and Sons, 1949.

18. Eucken, A., "Energy and Material Exchange on Boundary Surfaces," *Naturwissenschaften*, 25: 209-218, 1937.

19. Milne-Thomson, L. M., *Theoretical Hydrodynamics*. New York: The Macmillan Company, 1955.

20. Deissler, R. G., *Analysis of Turbulent Heat Transfer, Mass Transfer, and Friction on Smooth Tubes at High Prandtl and Schmidt Numbers*, Report No. 1210. Washington: National Advisory Committee for Aeronautics, 1955.

21. Rannie, W. D., *Heat Transfer in Turbulent Shear Flow*, PhD Thesis. Pasadena: California Institute of Technology, 1951.

22. Townsend, A. A., *The Structure of Turbulent Shear Flow*. Cambridge: Cambridge University Press, 1956.

23. Morse, P. M., and Feshbach, H., *Methods of Theoretical Physics*, vol. II. New York: McGraw-Hill Book Company, 1953.

APPENDIX

Velocity Due to a Two-Dimensional Array of Growing and Collapsing Bubbles

It is desired to calculate the velocity parallel to the wall of the liquid at any point between an array of growing and collapsing bubbles. The following assumptions are made:

1. The flow is irrotational, viscosity of the liquid being neglected.
2. The flow is two-dimensional, components perpendicular to the wall being neglected.
3. The bubbles can be considered to be point velocity sources and sinks, the distance between bubbles being large compared to their radii.
4. The bubbles can be considered to form an infinite, regular net of equal sources and sinks, the growth and collapse radius-time curves considered to be symmetrical. Each collapsing bubble will be surrounded by growing bubbles, so that the net can be represented as in Figs. 5 and 7, where L is the distance between adjacent bubble centers. We are thus interested in the potential distribution about an array of line sources, regularly spaced over the whole x,y plane. This potential is generated by taking the logarithm of an elliptic function, for such a function has zeros and simple poles regularly spaced on the complex plane. The spacing and distribution of the line charges in each cell will determine the elliptic function to be used. If, in addition, a uniform stream velocity v in the negative x direction, is superimposed, the appropriate potential term must be added. For the array given in Fig. 5, the complex velocity potential w is given by (Ref. 23):

$$w = 2me^{-\pi} \ln \left\{ \frac{\text{sn}\,(\omega,k)}{\text{sn}\,(\omega + k',k)} \right\} + Vz$$

$$= 2me^{-\pi} \ln \left\{ \frac{\text{sn}\,(\omega,k)\ \text{dn}\,(\omega,k)}{\text{cn}\,(\omega,k)} \right\} + Vz; \quad z = x + iy \tag{A-1}$$

where k is the modulus of the elliptic function, and k' is one-quarter of the real period. For a square net, $k' = 1.854$, and $k = 0.707$. The source strength m' for a line-source array of bubbles is

$$m' = (R\dot{R})_a \tag{A-2}$$

and

$$\omega = \frac{k'z}{L} \tag{A-3}$$

On the other hand, if the array is the sort given in Fig. 7, the potential is

$$w = 2m'e^{-\pi} \ln \left\{ \mathrm{cn}\,(\omega,k) \right\} + Vz \tag{A-4}$$

where now

$$\omega = \frac{\sqrt{2}k'z}{L} \tag{A-5}$$

The velocity u at any point z of the complex plane is found by differentiating the complex potential (Ref. 19)

$$u_b^2 = \left(\frac{dw}{dz}\right)\left(\frac{d\bar{w}}{d\bar{z}}\right) \tag{A-6}$$

where the bar here denotes the complex conjugate function. Equation (A-6), together with either Eq. (A-1) or (A-4), constitutes the solution of the problem.